Removal of Berth II Rock Pinnacle
Ketchikan, Alaska

Hydroacoustic Sound Source Verification Report

Prepared by:

Paul Donavan
Carrie Janello

January 23, 2020

ILLINGWORTH & RODKIN, INC.
Acoustics • Air Quality

INTRODUCTION

The City of Ketchikan, Alaska was authorized to conduct underwater confined blasting of a rock pinnacle and subsequent dredging to remove the blasted material in the Tongass Narrows, southeastern Alaska. Removal of the underwater pinnacle will expand the area of safe navigation depths for cruise ships that presently visit Berths I and II, as shown in Figure 1.

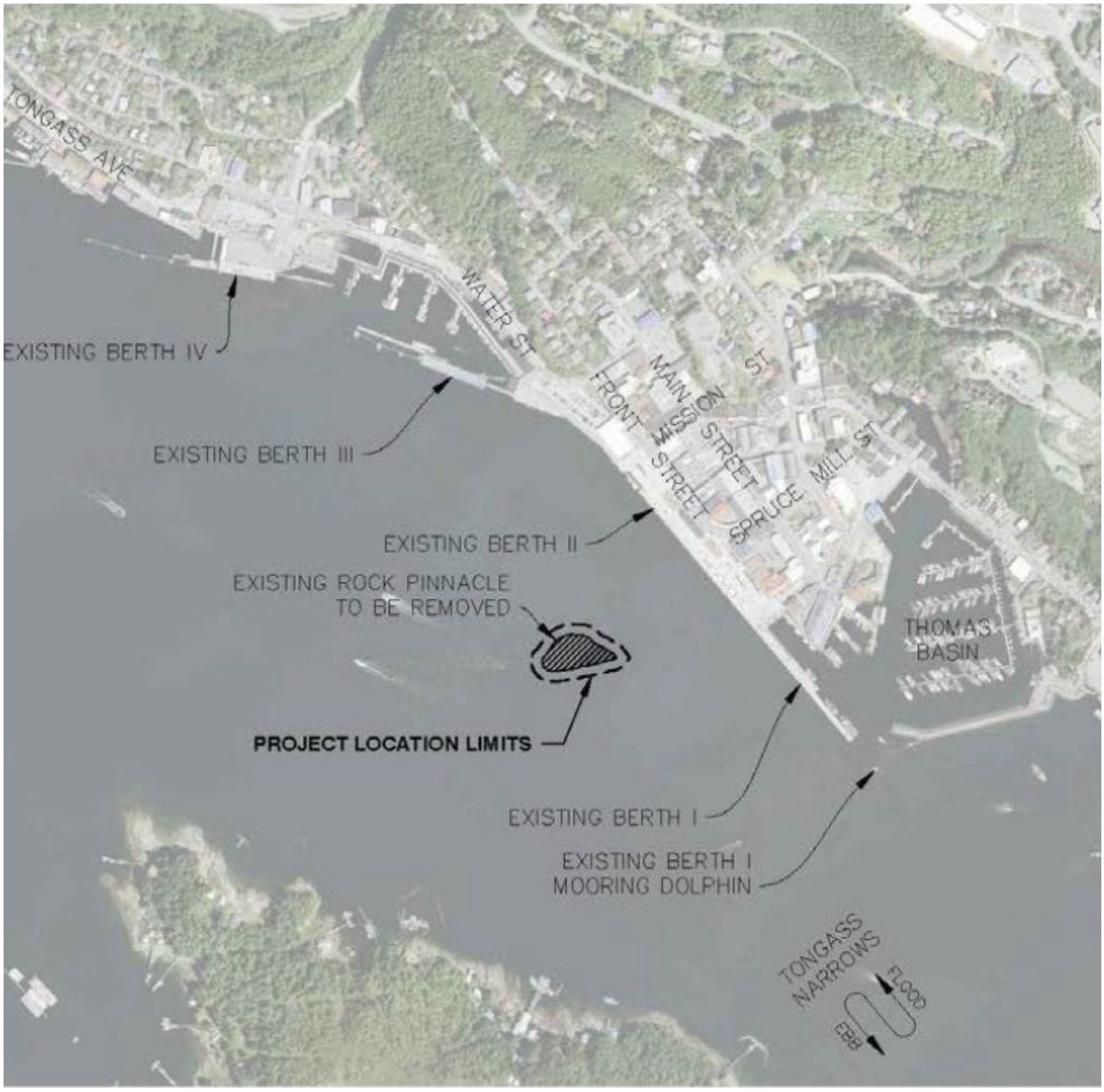

Figure 1: Rock pinnacle for removal and surrounding area, Ketchikan, Alaska

Removing the pinnacle will provide a more reliable ingress and egress for ships over a much wider range of wind and tide level conditions. The action has the potential to affect waters in the Tongass Narrows out to Revillagigedo Channel, approximately 3 miles to the south. The blasting began in mid-December 2019 and continued into January 2020.

Hydroacoustic monitoring was performed for the first four blasting events on each day between December 17, 2019 and December 20, 2019 in the vicinity of the rock pinnacle to verify the modeled isopleths. The four blast events included one test blast of a few holes and three additional full-strength blasts (20+ blast holes). Each of the monitored full-strength blasts was typical of the remaining planned blasting events, with one blast containing the maximum charge weight planned for the project. The purpose of this report is to document the hydroacoustic levels and blast pressures generated by these four blast events at different distances, as specified in the Special Conditions and Biological Opinion of the US Army Corps of Engineers Permit (No. POA-1922-00022-M26) and the Incidental Harassment Authorization (IHA) for the project..

Blast Plan

Blasting events occurred on four consecutive days between December 17, 2019 and December 20, 2019. Eight individual detonations were included in the first blasting event (Test Blast), while 21 to 22 were detonated in each of the remaining three full-strength blasting events (20+ blast holes each). Table 1 summarizes the number of detonations, charge weights, and time delays for each blasting event. Details pertaining to the blast plans on each day are documented in Appendix A.

Table 1: Charge weight information

Date of Event	Total Number of Charges	Charge Weights per Delay	Time Delay
December 17, 2019	8	26.9 lb	25 ms between holes single row
December 18, 2019	21	26.9 to 34.4 lb	25 ms between holes 84 ms between rows
December 19, 2019	22	26.9 to 41.9 lb	25 ms between holes 67 ms between rows
December 20, 2019	22	32.2 to 64.4 lb	25 ms between holes 67 ms between rows

Description of Measurement Metrics

The hydroacoustic pressure signals at each monitoring location were reduced and analyzed to obtain maximum peak pressure and sound pressure level (L_{pk}), cumulative sound exposure level (SELc), and root mean square (L_{RMS}) sound pressure levels. The pressure versus time signals from all monitoring locations were processed using the same algorithms to calculate the required metrics. Peak pressure level is defined as:

$$L_{pk} = 20\, Log_{10}\left(P_{pk}/P_{ref}\right) \qquad (1)$$

where L_{pk} is the peak level in dB, and P_{ref} is the reference pressure of 1 μPa. To calculate the cumulative SEL is given by:

$$SEL_{cum} = 10\, Log_{10}\left(\int_0^T \frac{P^2(t)\, dt}{P_{ref}^2}\right) \qquad (2)$$

where T is the duration of blast, $P^2(t)$ is the instantaneous pressure squared, and P_{ref} is the reference pressure of 1 μPa. The numerical calculation used for the analysis is calculated as a summation by the following equation:

$$SEL_{cum} = 10Log_{10}\left(\sum_{i=0}^{t}\frac{p_i^2}{p_{ref}^2}\Delta t_i\right) \quad (3)$$

where Δt_i is the time resolution of the pressure versus time signal, p_i^2 is the pressure squared in a specific increment of time, and t is the total duration of the blasting event. For the SEL in general, the limits or duration of the summation are hard to determine, as the waveform can contain both positive and negative pressures. The RMS level is given by:

$$p_{RMS} = \sqrt{\frac{1}{T_2-T_1}\int_{T_1}^{T_2} p^2\,(t)dt} \quad (4)$$

$$L_{RMS} = 20\ Log_{10}\left({p_{rms}}/{p_{ref}}\right) \quad (5)$$

where T_1 is the time at the beginning of the blasting event, and T_2 is the time at the end. Numerically, the RMS calculation is given by:

$$L_{RMS} = 20\ Log_{10}\left\{\sqrt{\frac{1}{T_2-T_1}\sum_{T_1}^{T_2} p_i^2\,\Delta t_i}\Big/ p_{ref}\right\} \quad (6)$$

Hydroacoustic Impact Assessment Criteria

National Marine Fisheries Service (NMFS) has developed acoustic thresholds that identify the received level of underwater sound above which exposed marine mammals would be reasonably expected to incur temporary threshold shifts (TTS; equated to Level B harassment) or permanent threshold shifts (PTS; equated to Level A harassment) of some degree.[1] Thresholds have also been developed to identify the pressure levels above which animals may incur different types of tissue damage from exposure to pressure waves from explosive detonation. Table 2 lists TTS, PTS, serious injury, and mortality thresholds for the five different species groups considered by NMFS.

Table 2. Explosive acoustic and pressure thresholds for marine mammals (84 FR 11508, March 27, 2019)

Group	Level B harassment		Level A harassment	Serious injury		Mortality
	Behavioral (multiple detonations)	TTS	PTS	Gastro-intestinal tract	Lung	
Low-freq cetacean	163 dB SEL	168 dB SEL or 213 dB SPL_{pk}	183 dB SEL or 219 dB SPL_{pk}	237 dB SPL	$39.1M^{1/3}$ $(1+[D/10.081])^{1/2}$ Pa-sec where: M = mass of the animals in kg D = depth of animal in m	$91.4M^{1/3}$ $(1+[D/10.081])^{1/2}$ Pa-sec where: M = mass of the animals in kg D = depth of animal in m
Mid-freq cetacean	165 dB SEL	170 dB SEL of 224 dB SPL_{pk}	185 dB SEL or 230 dB SPL_{pk}			
High-freq cetacean	135 dB SEL	140 dB SEL or 196 dB SPL_{pk}	155 dB SEL or 202 dB SPL_{pk}			
Phocidae	165 dB SEL	170 dB SEL or 212 dB SPL_{pk}	185 dB SEL or 218 dB SPL_{pk}			
Otariidae	183 dB SEL	188 dB SEL or 226 dB_{pk}	203 dB SEL or 232 dB SPL_{pk}			

In the Incidental Harassment Authorization (IHA) issued to the City of Ketchikan,[2] the modeled distances to the marine mammal criteria were for all species and criteria and are summarized in Table 3.

Table 3A: Model results of impact zones in feet documented in the Federal Register[2]

Marine Mammal Hearing Group	PTS: SELcum	PTS: SPLpk	TTS: SELcum	TTS: SPLpk
Low-Freq Cetacean	1411	617	7710	1230
Mid-Freq Cetacean	295	174	1411	348
High-Freq Cetacean	4659	4357	16404	8694
Otariidae	98	138	492	276
Phocidae	689	692	3675	1378

Table 3B: Model results of impact zones in meters documented in the Federal Register[2]

Marine Mammal Hearing Group	PTS: SELcum	PTS: SPLpk	TTS: SELcum	TTS: SPLpk
Low-Freq Cetacean	430	188	2350	375
Mid-Freq Cetacean	90	53	430	106
High-Freq Cetacean	1420	1328	5000	2650
Otariidae	30	42	150	84
Phocidae	210	211	1120	420

HYDROACOUSTIC MONITORING

Hydroacoustic monitoring occurred at up to five locations on each day of blasting. Pressure transducers were used at distances up to 500 feet due to the potential peak pressures that could occur. At 500 feet and beyond, hydrophone systems were used.

Monitoring Array

The nominal monitoring locations, which are shown in Figure 2, were about 200 to 1,200 feet from the blasting events. This monitoring array was submitted to NMFS prior to deployment. Pressure transducers were used at WM1 and WM2, and a hydrophone was used at WM5. Both types of sensors were used at WM3 and WM4, which were located at the same distance from the blasting event but at different depths. Sensors at WM1, WM2, WM3, and WM5 were positioned 10 feet below the water surface, while sensors at WM4 were positioned 10 feet above the floor of the water (at depth). An additional monitoring location (WM6), which was deployed from the dock at the closest distance to the blast, was made for the final blasting event. The water depth at this location was about 10 feet below the water surface.

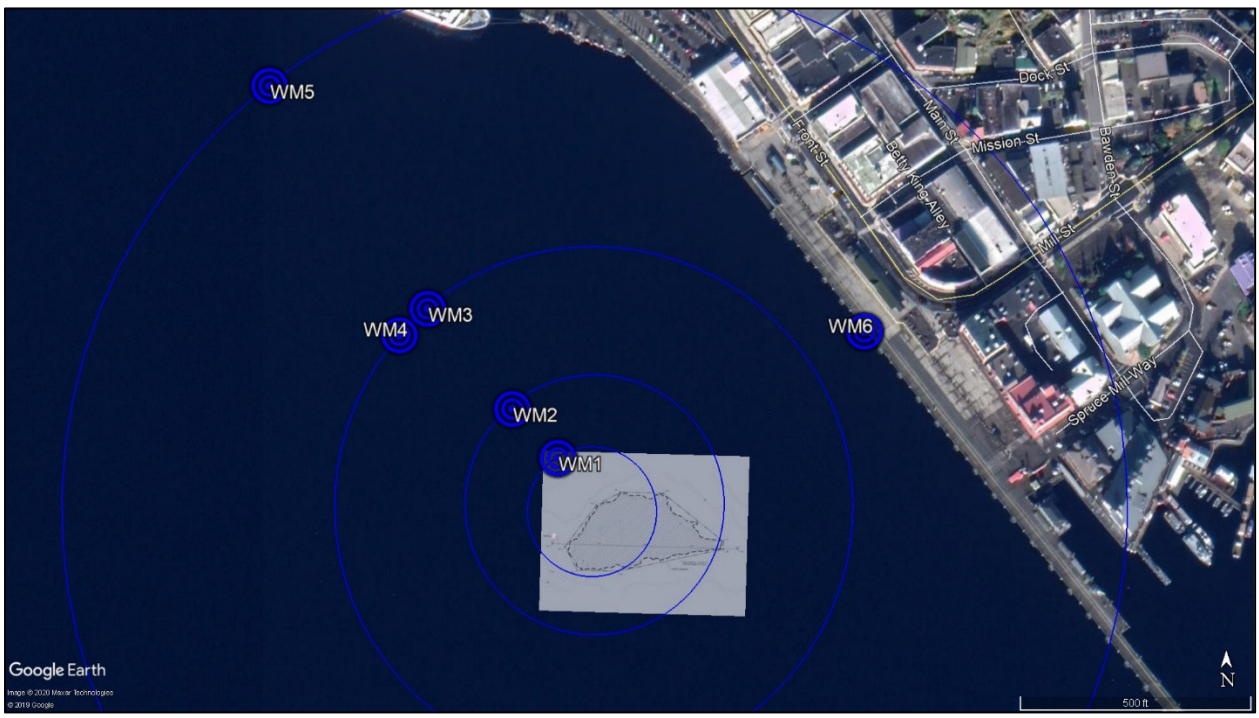

Figure 2: Nominal locations of all hydroacoustic monitoring

Instrumentation

Due to the nature of blasting events, the rise time of the pressure signals was short and required high speed acquisition of data. To meet this requirement, PCB Piezotronics, Inc. pressure sensor model number 138A01W transducers capable of measuring up to 1,000 psi were used in order to improve the measurement resolution. These transducers were capable of capturing signals of frequencies greater than 1,000 kHz and were used at WM1, WM2, WM3, and WM4. Each

transducer was input into a PCB Piezotronics, Inc. Model 482C05 four-channel ICP® Sensor Signal Conditioner. While there was no method for field calibration of these pressure transducers, all of the pressure transducers were calibrated by the manufacturer prior to shipment. Additionally, Teledyne Reson TC4013 hydrophones with upper frequency ranges of 170 kHz were also positioned at WM3 and WM4, as well as WM5 and WM6. For the hydrophones at WM3, WM4, and WM5, the signals from the hydrophones were input into Teledyne Reason EC6067 CCA 1000 conditioning charge amplifiers. Note, two hydrophones were deployed at WM5 on December 19, 2019 to ensure data was collected. The hydrophone system at WM6 was an autonomous unit, consisting of a TC4013 hydrophone, a PCB 422E13 charge converter, and a PCB 480E09 signal conditioner all housed in a water-tight cylindrical case about five inches in diameter and 12 inches long. Each of the hydrophone systems were field calibrated prior to the blasting events, as described below.

The voltage signals from all sensors at WM1 through WM4 were collected by an eight-channel high-speed transient data acquisition system (DAS) MREL DataTrap II Data recorder. The data was sampled at 1,000 kHz (one record per 0.001 milliseconds). A solid-state Roland R-05 audio recorder captured the hydrophone signals at WM5 and WM6. The sampling rate for this recorder was 96,000 samples per second.

Calibration

For the PCB 138A01W pressure transducers, there is no method of field calibration. The sensitivities supplied by the manufacturer were used to convert the measured voltages into pressure versus time. The accuracy of the MREL DataTrap II was supplied by the sources of the recorders.

For the TC4013 hydrophones, direct calibration was completed prior to each blasting event using a G.R.A.S. 42AC Pistonphone, high pressure, Class 1. This pistonphone was calibrated to produce a 165.3 dB sound pressure level at 250 Hz when used with a G.R.A.S. RA0078 Calibration Coupler for the TC4013. For systems using the Roland R-05 solid state recorder, the calibration tone was directly recorded and used to determine hydrophone sensitivities for the complete instrument chain. All sensitivities used on each day are summarized in Table 4.

Table 4: Summary of resultant sensitivities for each sensor

Blasting Event	Monitoring Location	Distance, ft	Measurement Transducer	Sampling Rate	Sensitivity
December 17, 2019	WM1	197	PCB	1 MHz	4.871 mV/psi
	WM2	341	PCB	1 MHz	4.965 mV/psi
	WM3	459	PCB	1 MHz	5.105 mV/psi
			Hydrophone	1 MHz	1,469.13 mV/psi
	WM4	459	PCB	1 MHz	5.091 mV/psi
			Hydrophone	1 MHz	1,403.47 mV/psi
	WM5	1,168	Hydrophone	96 kHz	163.654 mV/psi
December 18, 2019	WM1	205	PCB	1 MHz	4.871 mV/psi
	WM2	348	PCB	1 MHz	4.965 mV/psi
	WM3	466	PCB	1 MHz	5.105 mV/psi
			Hydrophone	1 MHz	1,469.13 mV/psi
	WM4	466	PCB	1 MHz	5. 091 mV/psi
			Hydrophone	1 MHz	1,403.47 mV/psi
	WM5	Data unavailable			
December 19, 2019	WM1	Data unavailable			
	WM2	438	PCB	1 MHz	4.965 mV/psi
	WM3	561	PCB	1 MHz	5.105 mV/psi
			Hydrophone	1 MHz	1,469.13 mV/psi
	WM4	561	PCB	1 MHz	5. 091 mV/psi
			Hydrophone	1 MHz	1,403.47 mV/psi
	WM5	1,191	Hydrophone	96 kHz	217.067 mV/psi
			Hydrophone	96 kHz	337.371 mV/psi
December 20, 2019	WM1	Data unavailable			
	WM2	Data unavailable			
	WM3	573	PCB	1 MHz	5.105 mV/psi
			Hydrophone	1 MHz	1,469.13 mV/psi
	WM4	573	PCB	1 MHz	5. 091 mV/psi
			Hydrophone	1 MHz	1,403.47 mV/psi
	WM5	1,207	Hydrophone	96 kHz	210.447 mV/psi
	WM6	985	Hydrophone	96 kHz	208.082 mV/psi

Data Capture and Processing

Data Capture

Data outputs from the DataTrap II were time histories (psi versus time) in text-file format. Signals captured by the Roland audio recorders were played back during post-processing into a high-speed Astro-Med, Inc. TMX multi-channel data acquisition system sampled at 200,000 samples/second. The TMX outputs were time histories (voltage versus time) in text-file format. Additionally, the recorded calibration tones were played into the high-speed recorder. These signals were used to calculate the sensitivities summarized above in Table 4.

To generate the representative Power Spectral Density (PSD) curves for the blasting events, the audio files recorded using the Roland units were played back into a Larson Davis Model 831 Sound Level Meter (SLM) setup for the Fast Fourier Transform (FFT) function. The output was exported into Microsoft Excel and converted into PSD form.

Data Processing

To compare with appropriate criteria, the pressure signals were reduced and analyzed to obtain peak pressure level, cumulative SEL, and RMS levels. The PCB transducers are designed to capture the true peaks in signals with rapid rise times and, as such, have excessive instrumentation noise. In order to produce comparable and usable results that are not artificially inflated by instrument noise, the PCB signals were processed using bandpass filters. Based on the signal, the high frequency filter cutoffs ranged from 30,000 Hz to 70,000 Hz. A low frequency filter cutoff of 10 to 20 Hz was used to eliminate low frequency excursions from zero that were not actually part of the blast signals. The hydrophone signals did not contain the high frequency noise found with the PCB transducers and did not require low pass filtering. The Roland recorders have internal high pass filtering at 100 Hz.

Data were all unfiltered (raw) and provided in psi for WM1 through WM4 monitoring locations and voltage for WM5 and WM6 locations. Optimum filter settings for the PCB signals were determined to report the peak pressures of the data in psi, and the data from WM5 and WM6 were converted into units of psi using the sensitivities shown in Table 3. All data were imported into National Instruments LabVIEW 2018. The pressure versus time signals were processed using the same algorithm to calculate the required metrics. The peak level and cumulative SEL_{cum} metrics were calculated numerically, as described above in this report. To calculate the 90% RMS, the filtered signals for the PCB sensors, which were generated in Labview, were exported into text-file format and imported into Microsoft Excel. Numerical calculations for the 90% RMS were made in Excel for each monitoring location. For all metrics, the psi values were converted into micro-Pascals (μPa) using 6.89×10^9 μPa/psi.

FISH OBSERVATIONS

One of the special conditions stated in the USACE permit was for the PSO to to immediately search the area down current of where SPL was expected to exceed 216 dB_{peak}, collect, and record dead fish on the three monitored full-strength blasts. The PSO was to discontinue the search after one hour since the currents in Tongass Narrows are strong. As time allows, the PSO was to search the area down current with predicted sound levels between 216 dB and 206 dB and record any fish mortality events (five or more dead fish) or fish at the surface with altered behavior (e.g. listing , sideways swimming, swimming in circles). The field observations of the PSO for each of the observed blasts are described in a separate report.

RESULTS OF HYDROACOUSTIC MONITORING

The blasting events occurred on December 17, 2019 at 12:13 p.m. AKST, on December 18, 2019 at 1:05 p.m. AKST, on December 19, 2019 at 12:00 p.m. AKST, and on December 20, 2019 at 12:03 p.m. AKST.

Analysis of Time Histories

Figure 3 shows an example of the time history (psi vs time) for the hydrophone at monitoring location WM4 for the Test Blast WB001 conducted on December 17, 2019. As shown in the figure, two distinct blasting sequences are observed. From -2200 to -1950 milliseconds (ms), the first element in the blast initiation sequence from the lead-in-line detonator and the subsequent micro-detonators which provided the millisecond delays between individual holes in the blast, were observed. These free-water isolated pressure peaks from the delay detonators were captured prior to each main blasting event between December 17, 2019 and December 20, 2020. The actual blast event to fracture the bedrock occurred between -1700 and -1350 ms. All time histories for each day and at each monitoring location are shown in Appendix B.

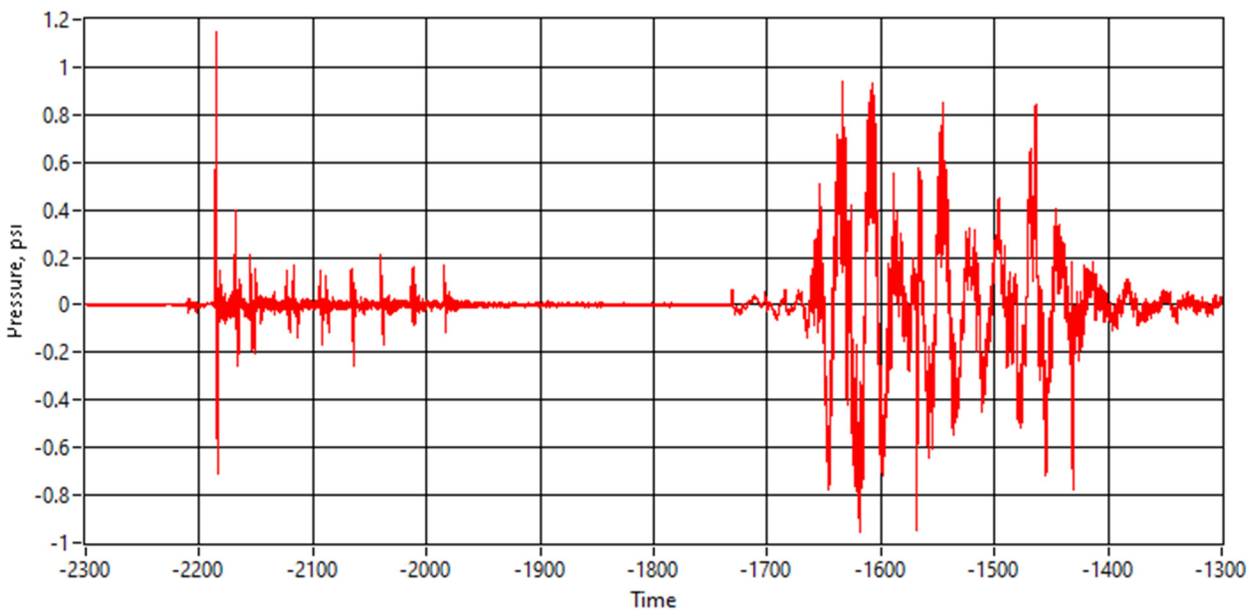

Figure 3: Time history for the hydrophone sensor at WM4 on December 17, 2019

As shown in Figure 3, the overall peak at WM4 occurred during the initiation of the blasting sequence; however, the main test blast event included more overall energy in each of the peaks than observed from the initiating detonators. The reporting requirements for this project included maximum peak levels and SELs for each individual blast cap in the event. On December 17, 2019, the main test blast portion of the WM4 location, which is isolated in Figure 4, can be dissected to show the eight individual detonations. However, it is difficult to determine when response is due to an individual detonation and when it is a continued response from a previous detonation. Figure 5, for instance, shows data captured at WM4 from the production blast on December 18, 2019 when 21 individual detonations occurred. Determining the peak levels and SELs for 21 individual detonations is not feasible. Further, the high frequency electrical interference in the PCB data

makes it even harder to determine what peaks were due to detonations from individual blasts. Therefore, peak levels, SEL_{cum}, and 90% RMS were determined separately for the entire events (initiation + bedrock blasts) and for the bedrock blast sequence only. Peak levels and SELs for individual blasts in the sequence were not calculated for this project.

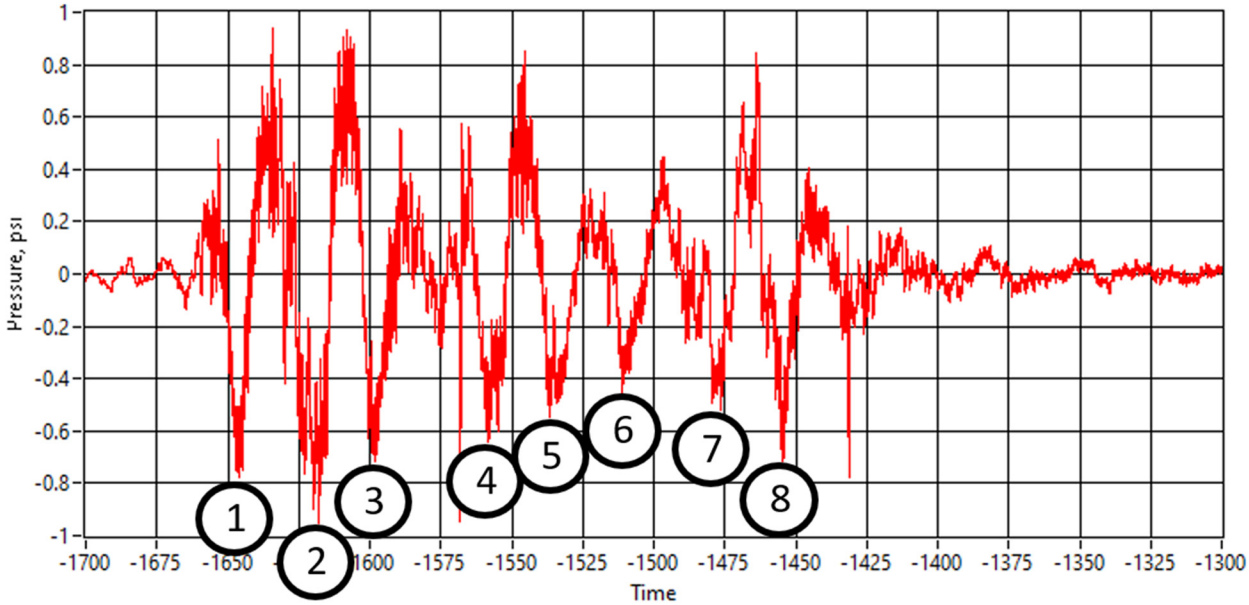

Figure 4: Time history for the hydrophone sensor at WM4 on December 17, 2019 during the bedrock blast only

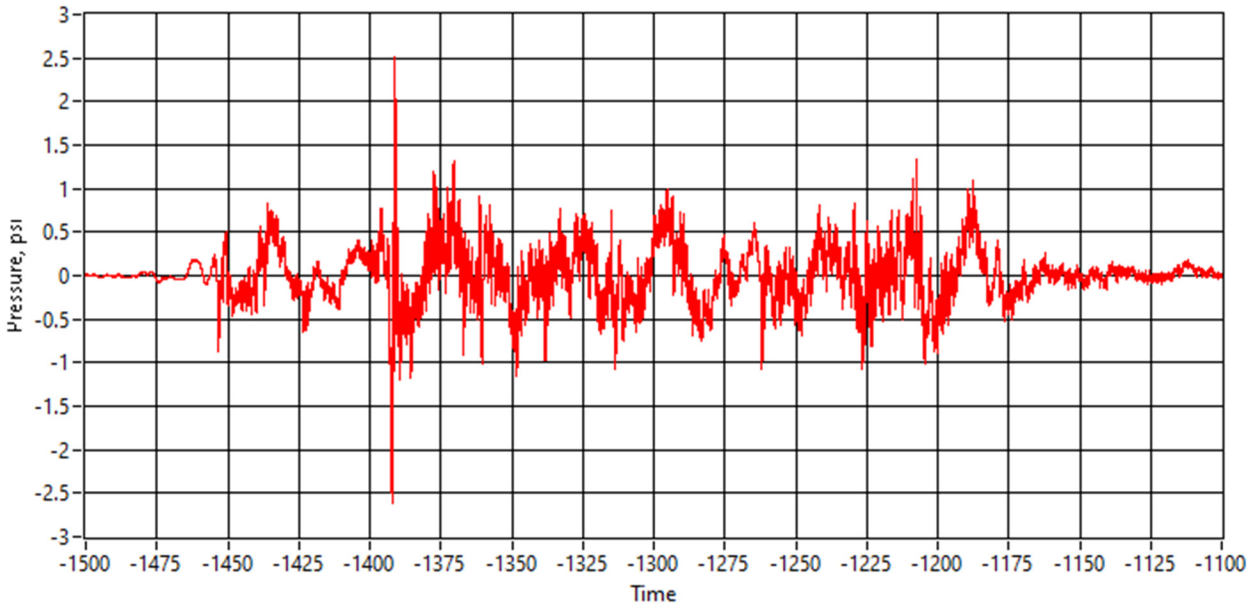

Figure 5: Time history for the hydrophone sensor at WM4 on December 18, 2019 during bedrock blasting only

Figure 6 shows the sound pressure distribution (in decibels) for WM4 on December 17, 2019. Both the initiation and main test blast event are shown in Figure 6. While the initial peak of the initiation

detonators shows a similar peak value than the main bedrock blasting event, the energy included in the main test blast event is considerably greater than the initiation portion.

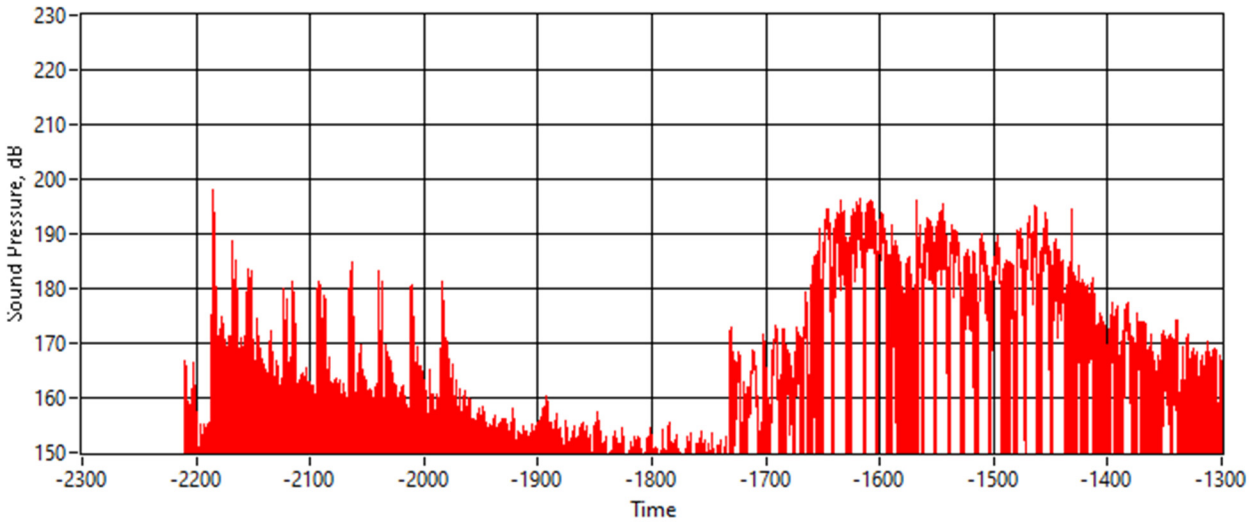

Figure 6: Sound pressure levels for the hydrophone sensor at WM4 on December 17, 2019

Summary of Results

Using the methods discussed above, the monitoring results for each location on December 17, 2019, December 18, 2019, December 19, 2019, and December 20, 2019 are presented in Tables 5 through 8, respectively. The values include peak pressure in psi, peak sound pressure level in dB, SELc in dB, and 90% RMS pressure level in dB.

Table 5: Summary of monitoring results from December 17, 2019

Monitoring Location	Distance, ft	Results for Entire Blasting Event				Results for Bedrock Blasting Only			
		Peak Level, psi	Peak Level, dB	SELcum, dB	90% RMS, dB	Peak Level, psi	Peak Level, dB	SELcum, dB	90% RMS, dB
WM1	197	4.441	209.7	186.0	187.0	3.340	207.2	185.7	190.9
WM2	341	2.332	204.1	181.1	181.7	1.460	200.1	180.2	185.3
WM3, PCB	459	2.374	204.3	179.1	179.6	1.541	200.5	177.8	183.0
WM3, Hydrophone	459	0.865	195.5	170.5	176.2	0.744	194.2	170.4	176.3
WM4, PCB	459	2.642	205.2	186.1	191.8	2.360	204.2	186.0	195.5
WM4, Hydrophone	459	1.147	198.0	180.8	187.5	0.955	196.4	180.7	187.4
WM5	1,168	0.6398	192.9	169.0	173.7	0.4832	190.5	168.8	173.4

Table 6: Summary of monitoring results from December 18, 2019

Monitoring Location	Distance, ft	Results for Entire Blasting Event				Results for Bedrock Blasting Only			
		Peak Level, psi	Peak Level, dB	SELcum, dB	90% RMS, dB	Peak Level, psi	Peak Level, dB	SELcum, dB	90% RMS, dB
WM1	205	5.569	211.7	189.9	195.4	5.569	211.7	189.5	195.5
WM2	348	3.576	207.8	186.2	186.9	3.576	207.8	185.4	190.7
WM3, PCB	466	2.103	203.2	183.7	183.7	2.103	203.2	182.7	187.0
WM3, Hydrophone	466	0.964	196.5	176.0	181.5	0.964	195.5	175.9	181.6
WM4, PCB	466	4.983	210.7	187.4	191.9	4.983	210.7	187.2	195.2
WM4, Hydrophone	466	2.616	205.1	182.3	187.9	2.616	205.1	182.3	187.9
WM5	Data unavailable								

Table 7: Summary of monitoring results from December 19, 2019

Monitoring Location	Distance, ft	Results for Entire Blasting Event				Results for Bedrock Blasting Only			
		Peak Level, psi	Peak Level, dB	SELcum, dB	90% RMS, dB	Peak Level, psi	Peak Level, dB	SELcum, dB	90% RMS, dB
WM1	Data unavailable								
WM2	438	6.428	212.9	187.0	190.9	6.428	212.9	186.7	191.1
WM3, PCB	561	3.772	208.3	182.4	182.7	3.772	208.3	181.8	185.9
WM3, Hydrophone	561	1.829	202.0	175.7	179.9	1.829	202.0	175.6	179.9
WM4, PCB	561	6.521	213.1	188.4	192.6	6.521	213.1	188.3	192.7
WM4, Hydrophone	561	3.534	207.7	182.7	187.0	3.534	207.7	182.6	187.0
WM5a	1,191	1.206	199.8	175.6	178.8	1.206	199.8	175.6	178.8
WM5b	1,191	1.238	200.8	176.2	179.4	1.238	200.8	176.2	179.3

Table 8: Summary of monitoring results from December 20, 2019

Monitoring Location	Distance, ft	Results for Entire Blasting Event				Results for Bedrock Blasting Only			
		Peak Level, psi	Peak Level, dB	SELcum, dB	90% RMS, dB	Peak Level, psi	Peak Level, dB	SELcum, dB	90% RMS, dB
WM1	Data unavailable								
WM2	Data unavailable								
WM3, PCB	573	11.32	217.9	187.4	188.0	11.32	217.9	186.5	191.6
WM3, Hydrophone	573	3.442	207.5	179.3	184.3	3.442	207.5	179.2	184.3
WM4, PCB	573	9.281	216.1	191.5	195.6	9.281	216.1	191.2	195.7
WM4, Hydrophone	573	3.63	208.0	185.6	190.1	3.63	208.0	185.5	189.6
WM5	1,207	1.145	198.2	176.6	180.5	1.145	198.2	176.6	180.5
WM6	985	1.88	202.3	173.2	178.5	1.88	202.3	173.1	178.4

The differences in the SEL_{cum} for the full signal versus the bedrock blasting only was less than 1 dB, except at the WM3 PCB sensor on December 17, 2019 when a difference of 1.3 dB occurred. This indicates that the majority of the overall energy from each blasting event occurred during bedrock blasting, with the initiating detonators accounting for less than 1 dB of the total energy.

For the 90% RMS levels, the full blasting event was typically within 1 dB of the 90% RMS for the bedrock blasting only; however, for some sensors, the 90% RMS was up to 3.9 dB higher for the bedrock blasting only than for the full event. This would be due to the time duration of the 90%. The shorter the time, the higher the level. When a longer time period is considered, such was the case for the full event, the level would decrease.

Since most of the energy occurred from bedrock blasting only, these levels are used in the subsequent analysis. Ninety percent of the total energy in the blasts occurred in time durations ranging from 0.1924 to 0.4329 seconds for every sensor and every event.

Power Spectral Density Curves

The recordings made at the distant monitoring locations were also processed using a Fast Fourier Transform (FFT), and the FFT was used to determine the power spectral density (PSD) curves for the distant signals. Additionally, the PSD curve was determined for the WM6 location, as well. The power spectrum of a time series describes the distribution of power into frequency components composing that signal. The PSD shows the power content at every frequency from 1 to 20,000 Hz. Figure 7 shows the PSD curve at WM5 on December 17, 2019. All remaining PSD plots are provided in Appendix C.

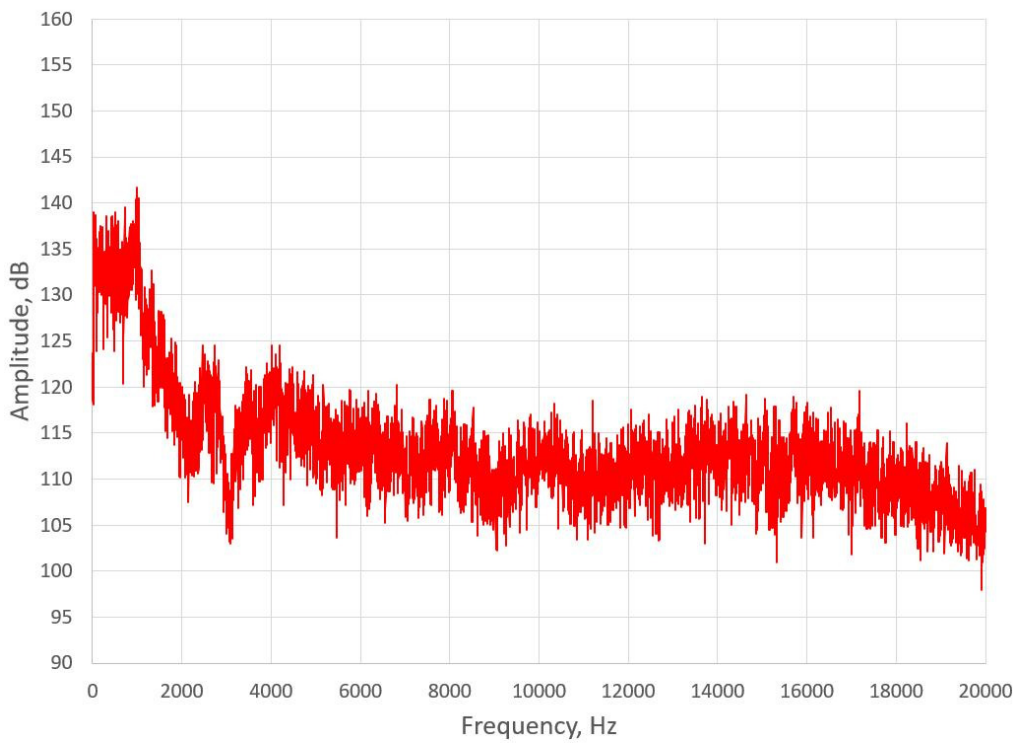

Figure 7: Power Spectral Density for the WM5 monitoring location on December 17, 2019

COMPARISON OF RESULTS TO CRITERIA

To determine the distances to these criteria, the measured SEL_{cum} values were used to determine the rate at which the levels decrease with distance. For this purpose, only the data from the 10-foot depth was used, and the data from the dock location on December 20th was excluded. The measured, unweighted SEL_{cum} values for each of the four blast events are plotted in Figure 8, as a function of distance along with the corresponding logarithmic trend line. The falloffs included in

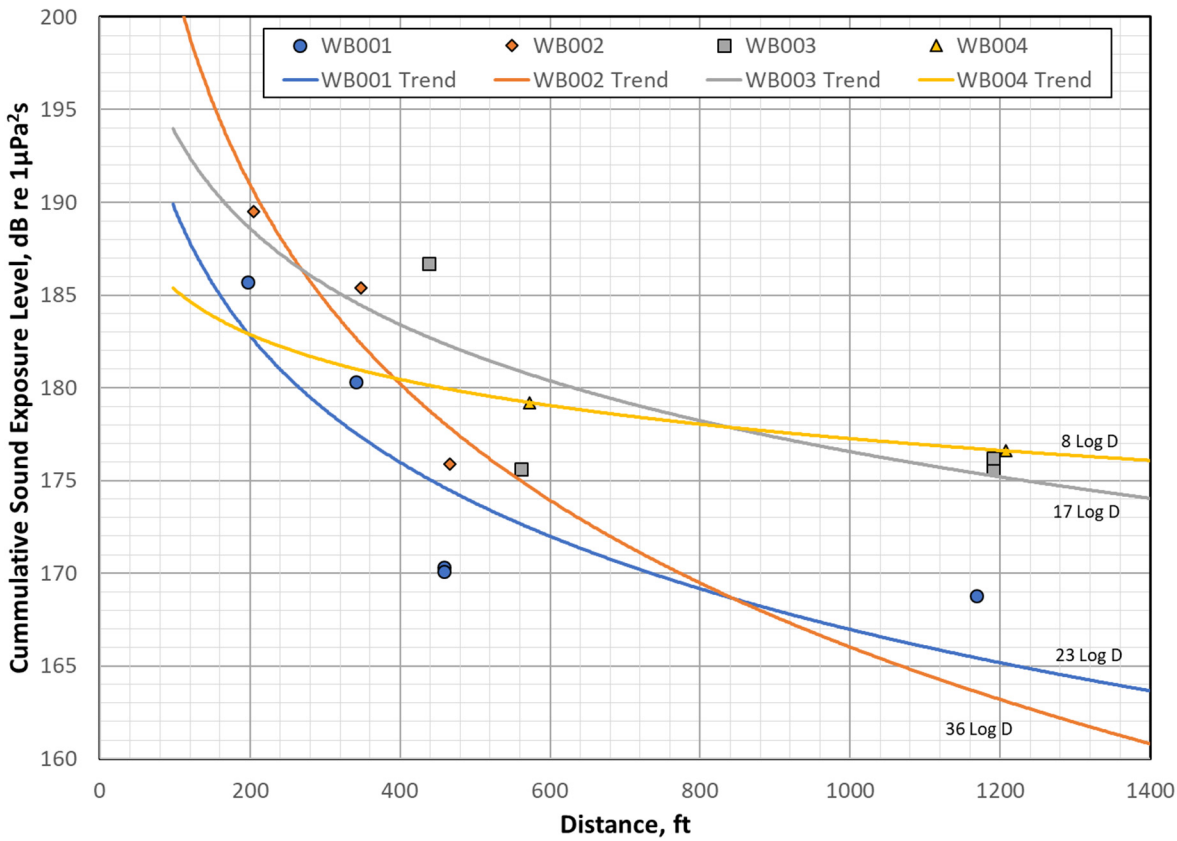

Figure 8: SELc levels for all blast events with indicated falloff rates

Figure 8 are significantly different, ranging from 8 Log D to 36 Log D. As would be expected from the blast plans, the levels for WB001 test blast on December 17, 2019 are consistently lower than the other production blasts. With the limited data and the exclusion of the WB001 initiation portion, the SEL_{cum} trend lines are still not consistent from one event to another. To establish a fall-off rate that could be used to determine the distances to criteria, a trend line for the SEL_{cum} values for each of the production blasts WB002 to WB004 was produced, as shown in Figure 9. This trend line was then uniformly increased by 1.2 dB so that it would pass through the average of the levels at 1,200 feet, as also shown in Figure 9. These trend lines have a fall-off rate of 16.5 Log distance. These data were then weighted by the factors appropriate for each of the five marine mammal species groups. The same process was completed for the peak sound pressure level and is shown in Figure 10. These data produced a falloff rate of 15.4 Log D.

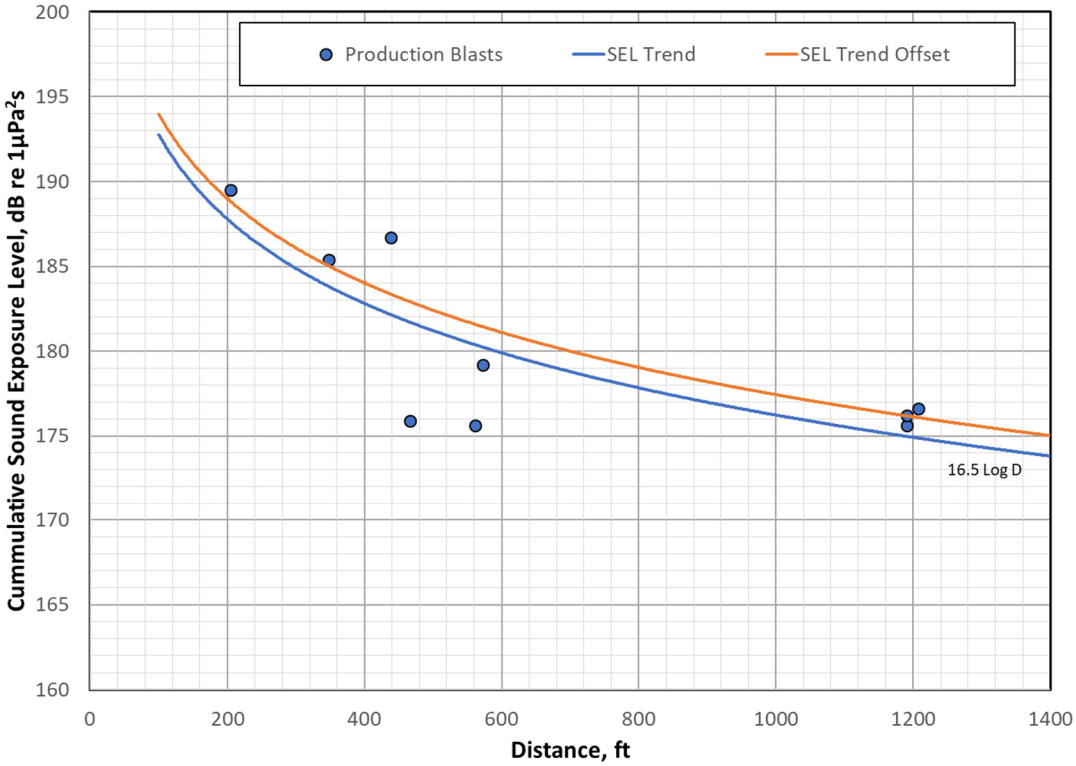

Figure 9: SEL_{cum} data and fall-off trend line for production blasts WB002, WB003, and WB004

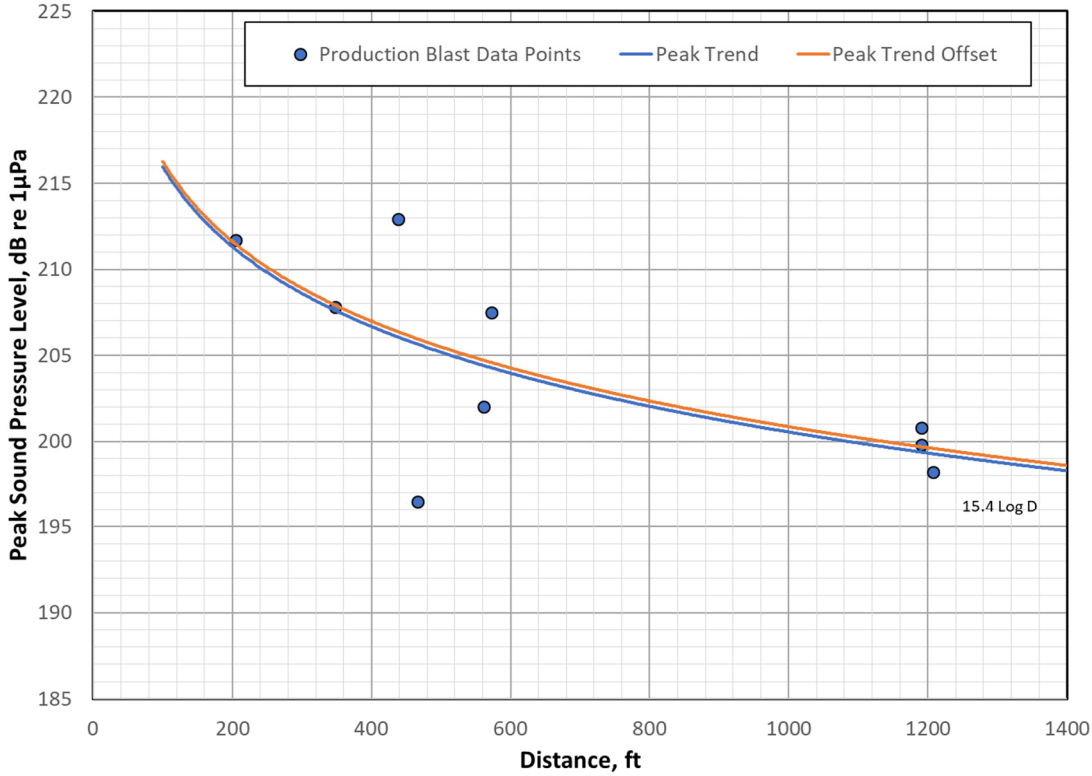

Figure 10: L_{pk} data and fall-off trend line for production blasts WB002, WB003, and WB004

The peak sound pressure levels do not require weighting, however, as the effect on different species is accounted for in the criteria level set for each species.

Using the level versus distance fall-off rates as determined above, the distances to the Level A and Level B criteria were determined for each species, as shown in Table 9.

Table 9: Measured distances to Marine Mammal criteria for Production Blasts

Marine Mammal Hearing Group	**Distance to Criteria, feet**				
	Level A Harassment		**Level B Harassment**		
	SEL (PTS)	**Peak (PTS)**	**SEL (TTS)**	**Peak (TTS)**	**SEL Behavioral**
Low-Freq Cetacean	287	66	2028	163	2999
Mid-Freq Cetacean	42	13	266	32	493
High-Freq Cetacean	1354	842	8601	2064	15929
Otariidae	11	10	74	23	139
Phocidae	112	77	728	189	1359

For all species and criteria, the distances determined from the measurements are less than those of modeled results reported in Table 3 from the IHA (as an easy reference, the table below is a copy of Table 3 on page 5 of this report).[2]

Table 3A: Model results of impact zones in feet documented in the Federal Register[2]

Marine Mammal Hearing Group	PTS: SELcum	PTS: SPLpk	TTS: SELcum	TTS: SPLpk
Low-Freq Cetacean	1411	617	7710	1230
Mid-Freq Cetacean	295	174	1411	348
High-Freq Cetacean	4659	4357	16404	8694
Otariidae	98	138	492	276
Phocidae	689	692	3675	1378

Table 3B: Model results of impact zones in meters documented in the Federal Register[2]

Marine Mammal Hearing Group	PTS: SELcum	PTS: SPLpk	TTS: SELcum	TTS: SPLpk
Low-Freq Cetacean	430	188	2350	375
Mid-Freq Cetacean	90	53	430	106
High-Freq Cetacean	1420	1328	5000	2650
Otariidae	30	42	150	84
Phocidae	210	211	1120	420

REFERENCES

1. NMFS's Technical Guidance for Assessing the Effects of Anthropogenic Sound on Marine Mammal Hearing (Version 2.0). Available at (Accessed June 5, 2019): https://www.fisheries.noaa.gov/national/marine-mammal-protection/marine-mammal-acoustic-technical-guidance
2. **Federal Register** /Vol. 84, No. 146 /Tuesday, July 30, 2019 pp36891-36904 /Notices https://www.govinfo.gov/content/pkg/FR-2019-07-30/pdf/2019-16155.pdf

APPENDIX A1: BLAST PLAN --- TEST BLAST

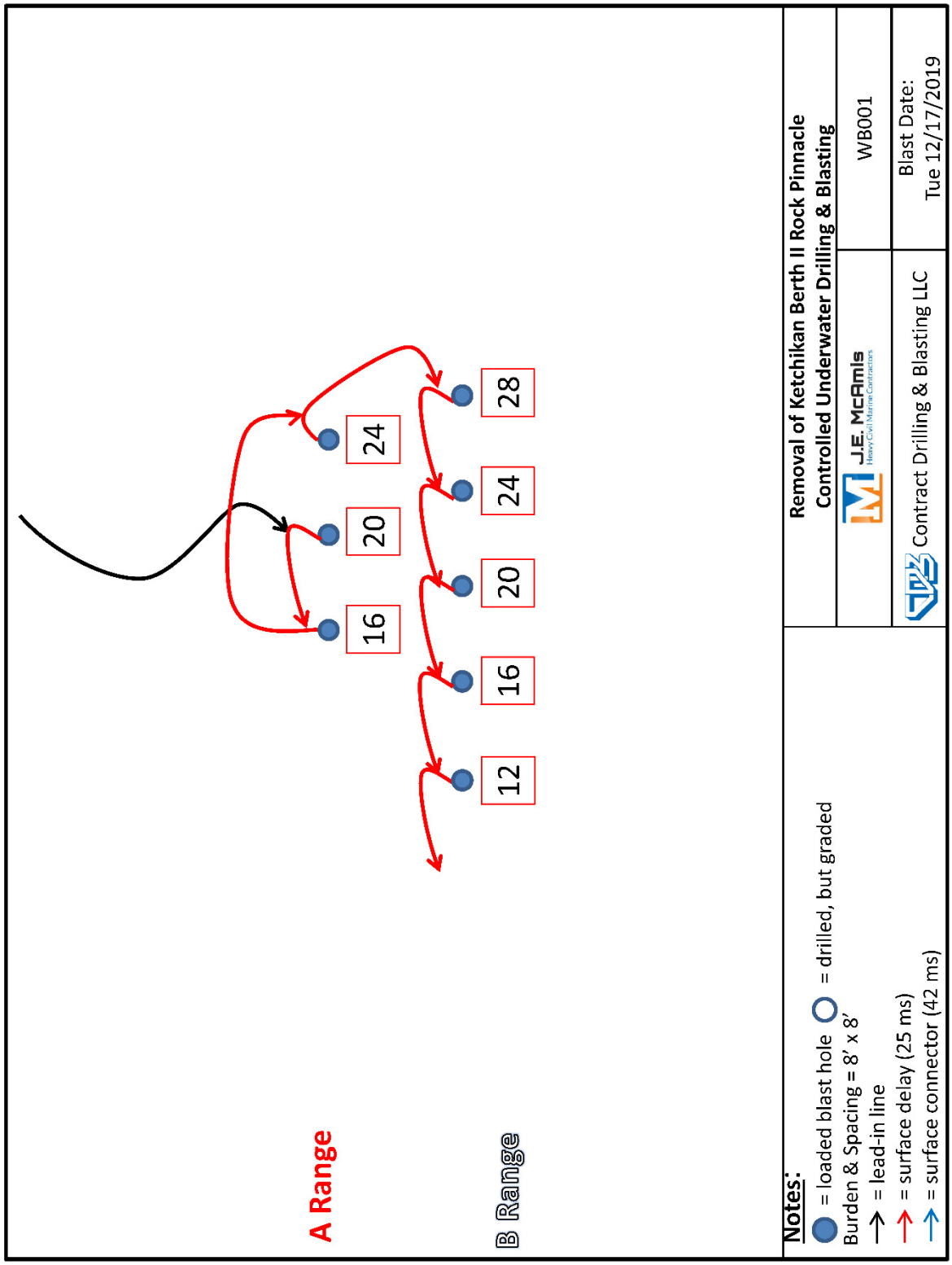

APPENDIX A2: BLAST PLAN --- FULL-STRENGTH BLAST 1 (20+ BLAST HOLES)

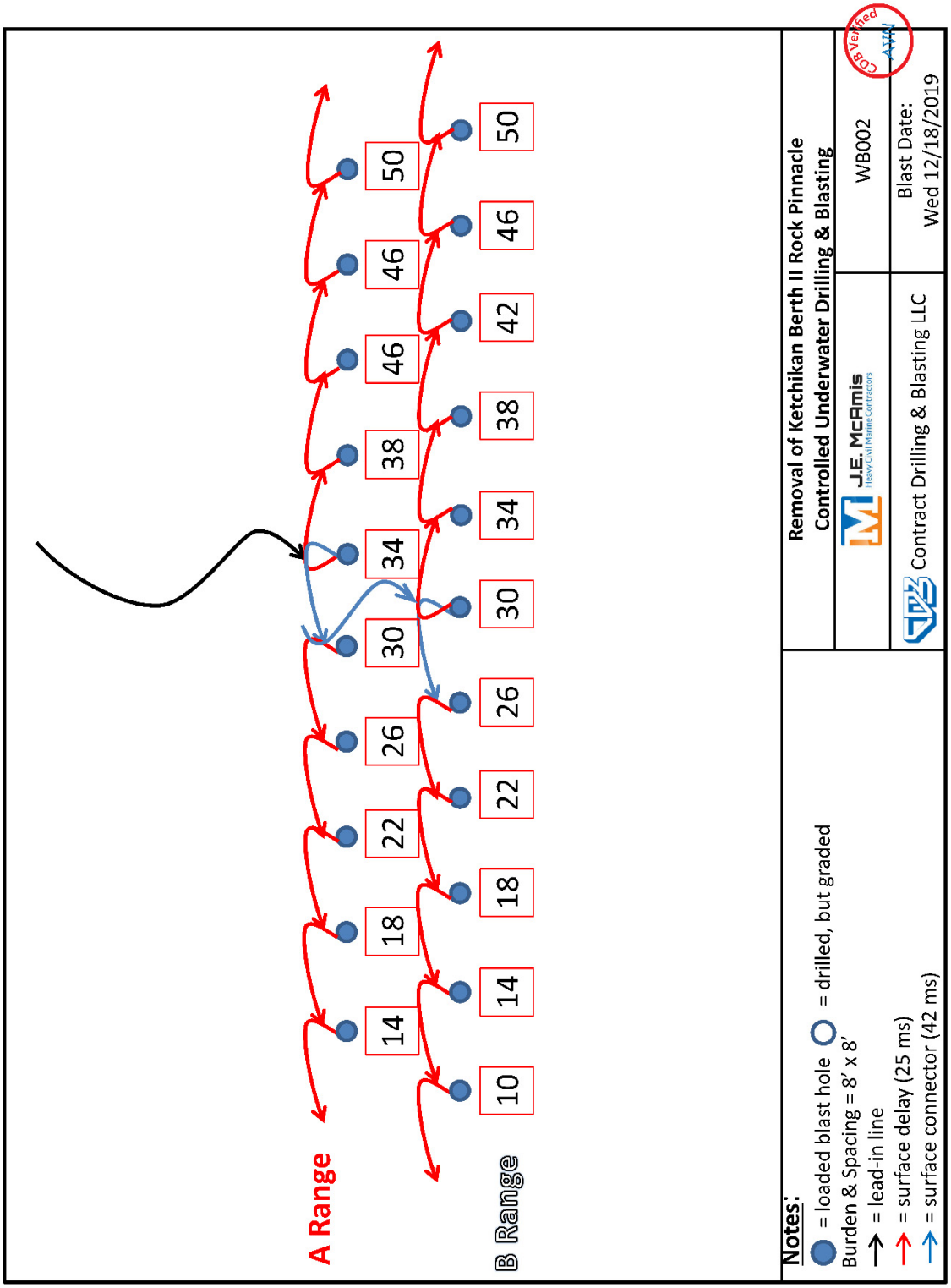

APPENDIX A3: BLAST PLAN --- FULL-STRENGTH BLAST 2 (20+ BLAST HOLES)

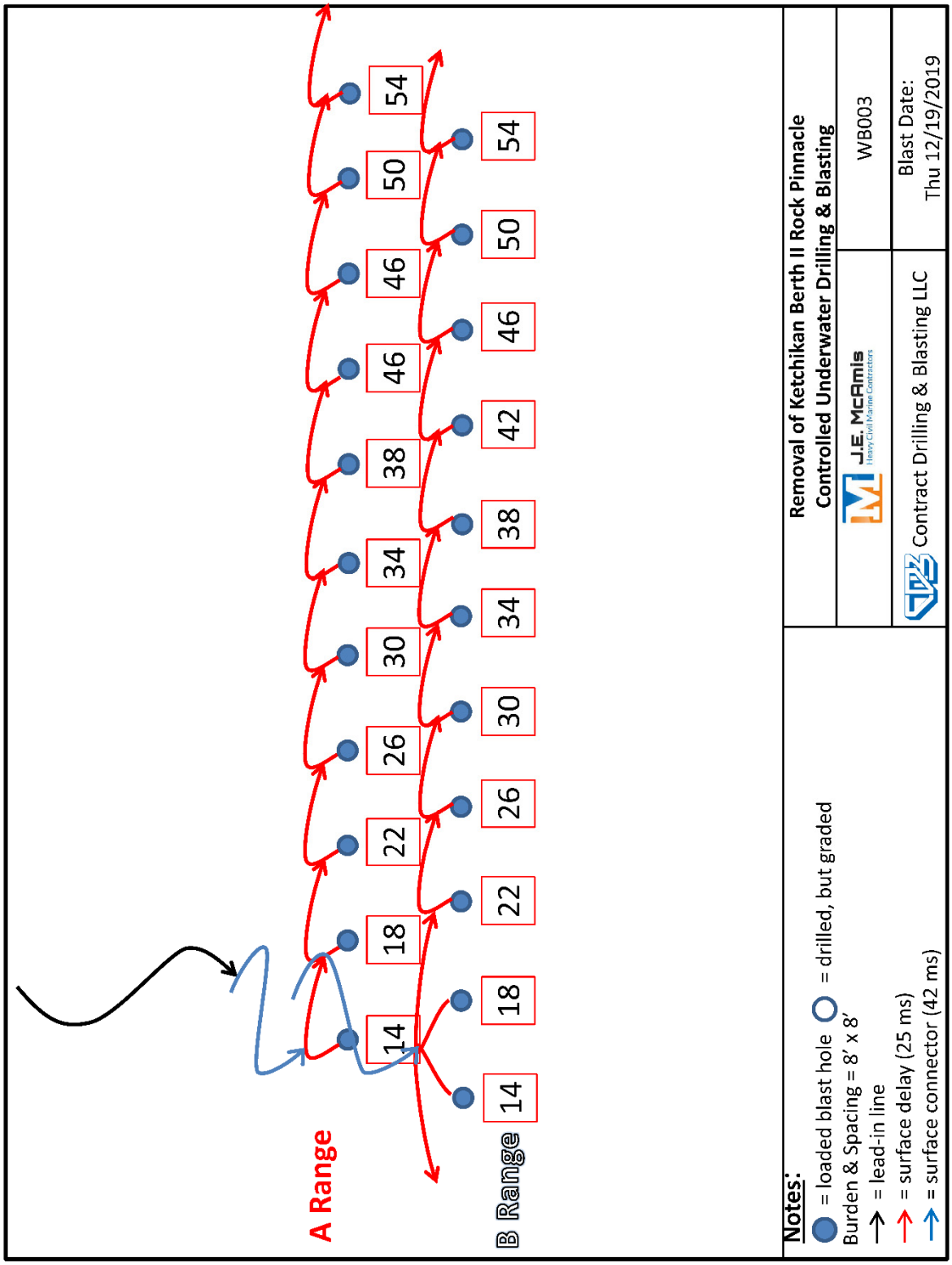

APPENDIX A4: BLAST PLAN --- FULL-STRENGTH BLAST 3 (20+ BLAST HOLES)

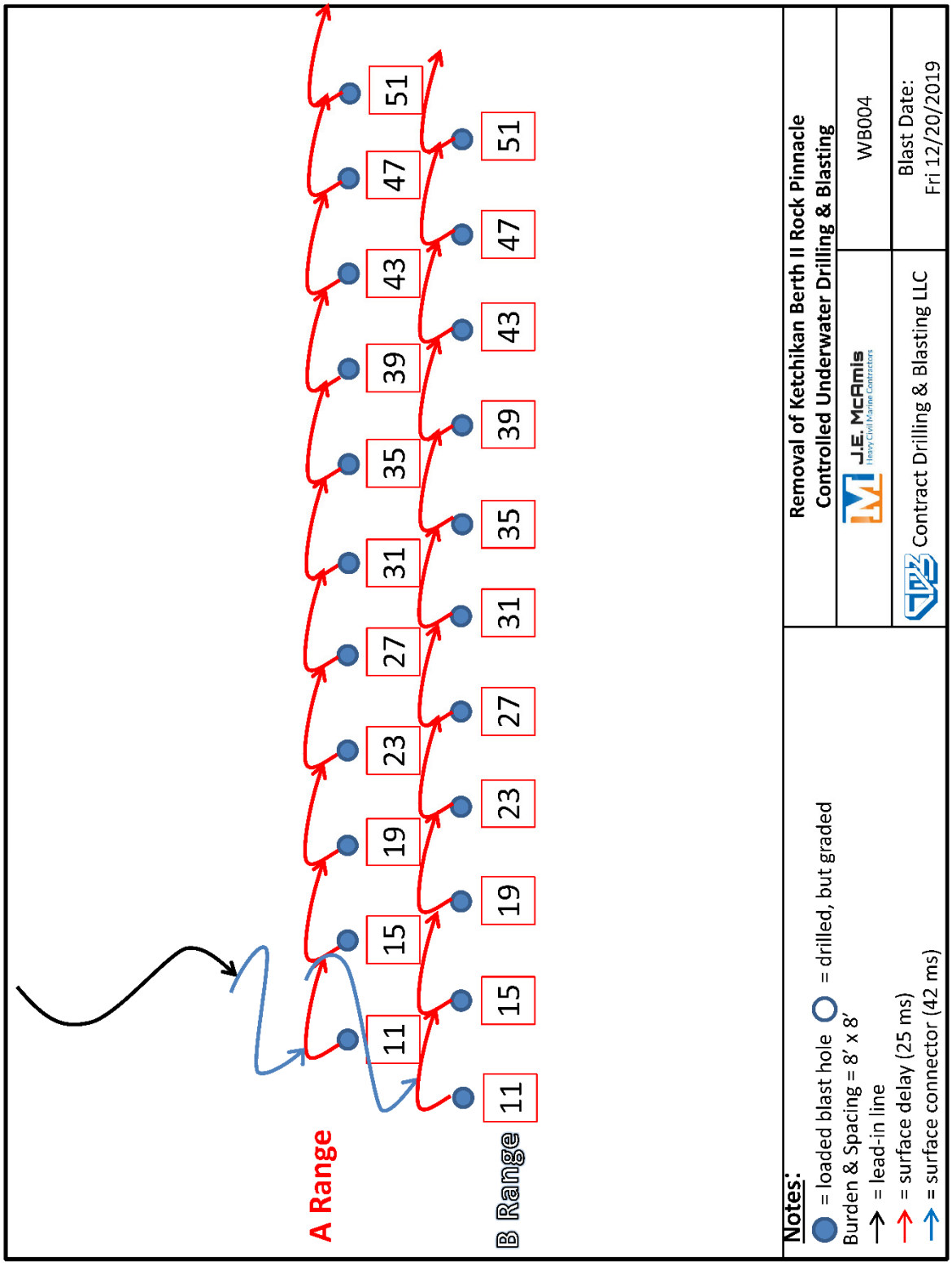

APPENDIX B: RESULT FIGURES

December 17, 2019

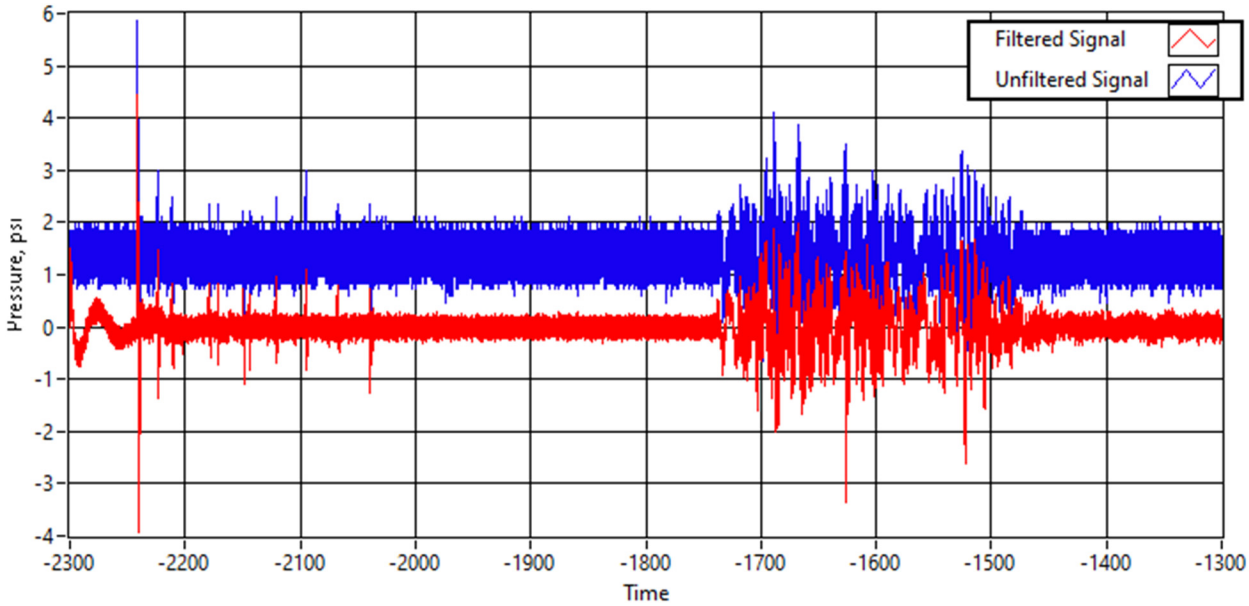

Figure B1: Time history for the PCB sensor at WM1 on December 17, 2019

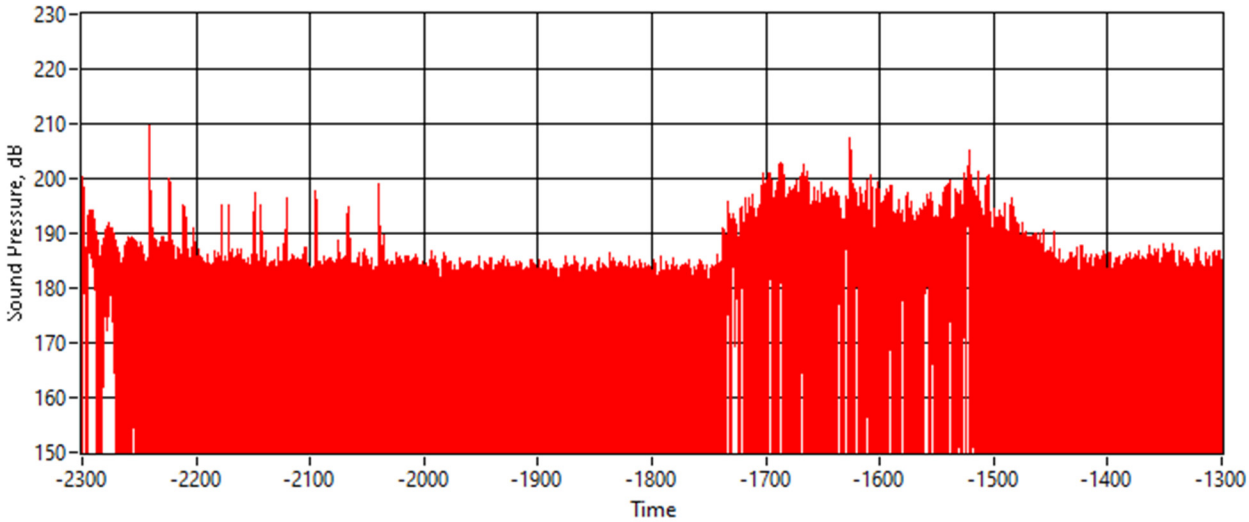

Figure B2: Sound pressure levels for the PCB sensor at WM1 on December 17, 2019 (filtered only)

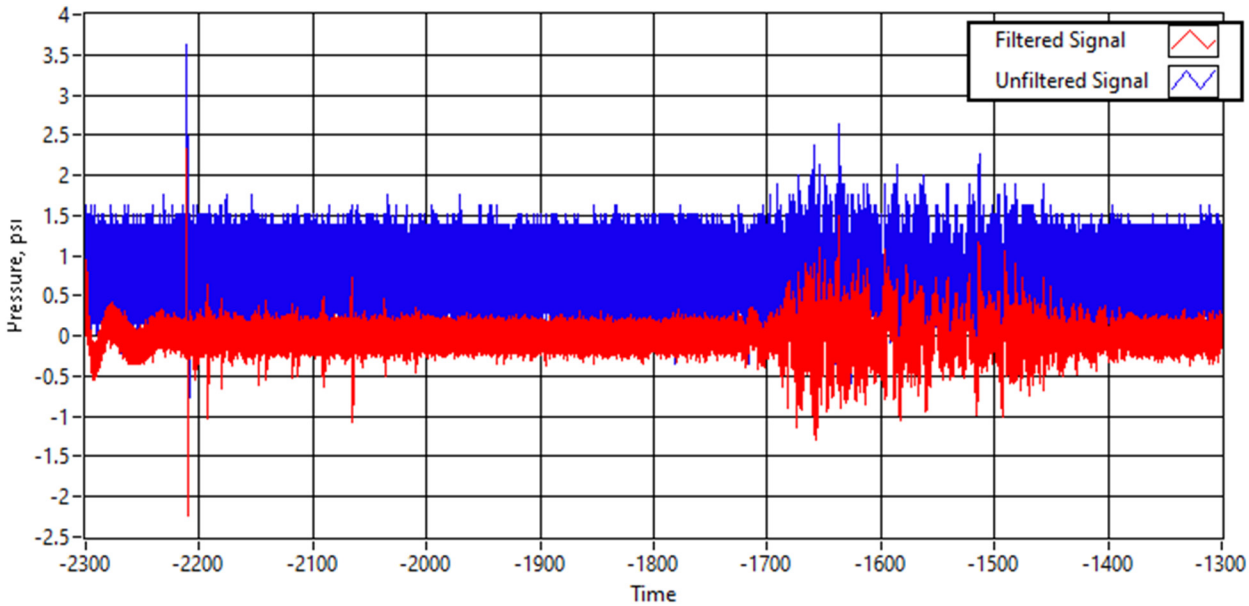

Figure B3: Time history for the PCB sensor at WM2 on December 17, 2019

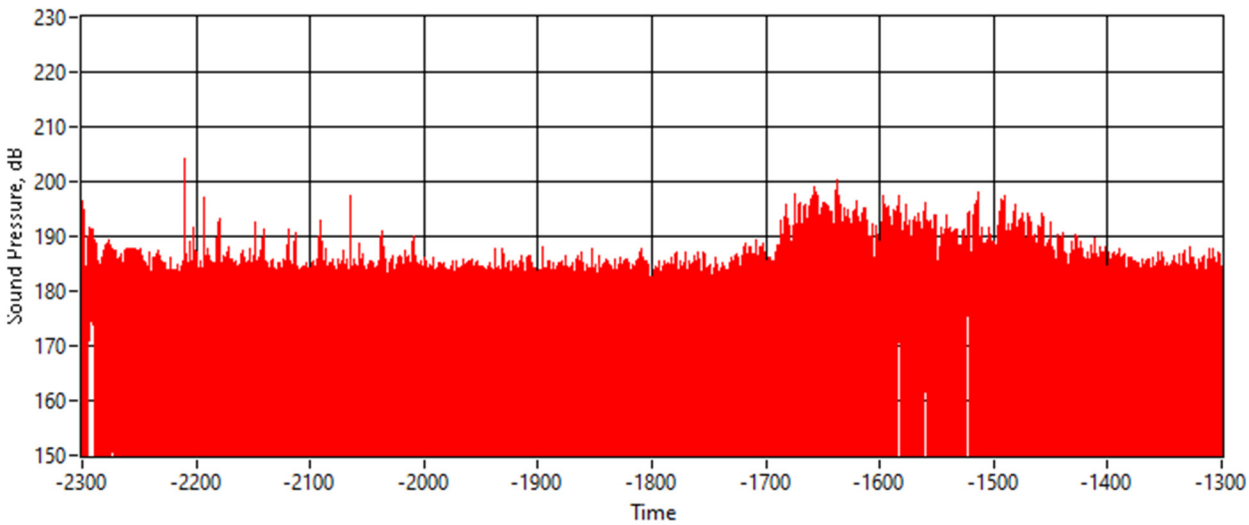

Figure B4: Sound pressure levels for the PCB sensor at WM2 on December 17, 2019 (filtered only)

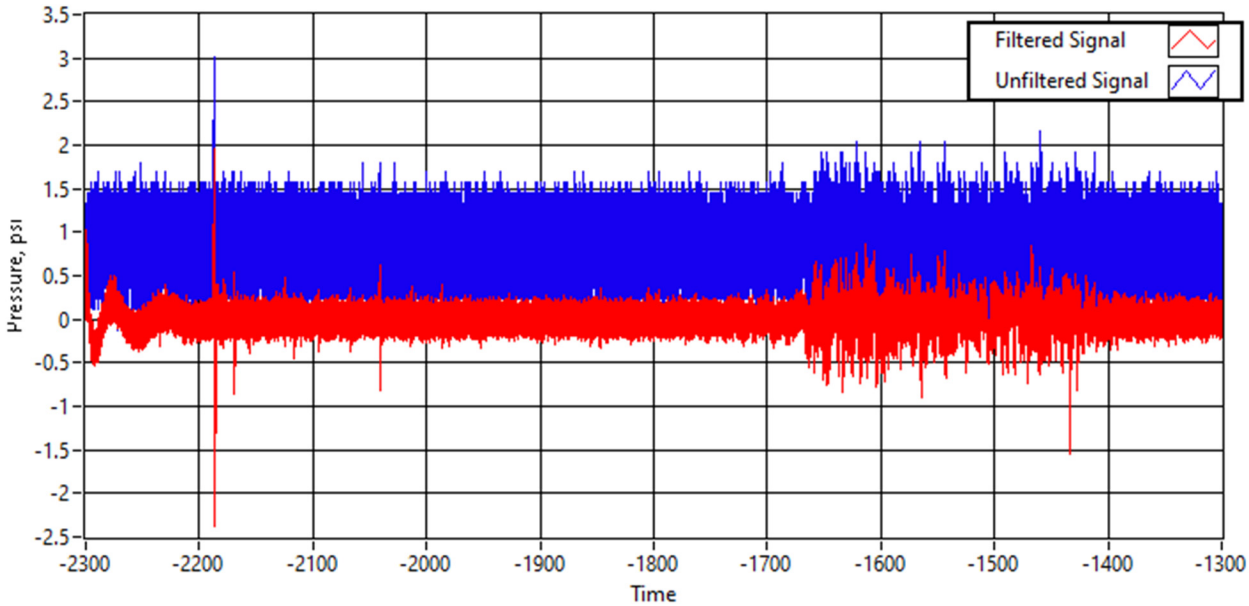

Figure B5: Time history for the PCB sensor at WM3 on December 17, 2019

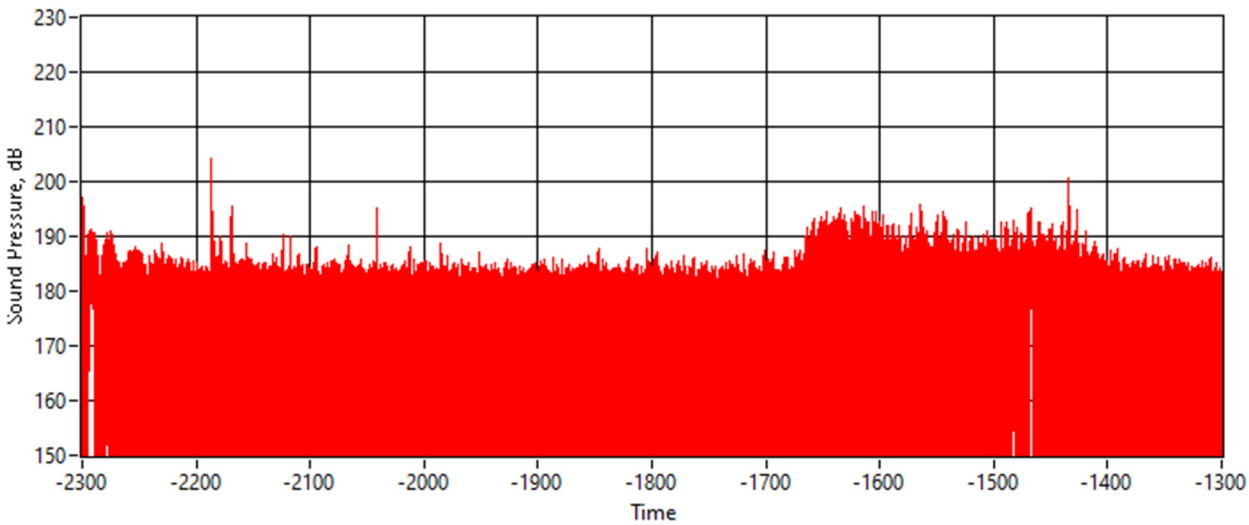

Figure B6: Sound pressure levels for the PCB sensor at WM3 on December 17, 2019 (filtered only)

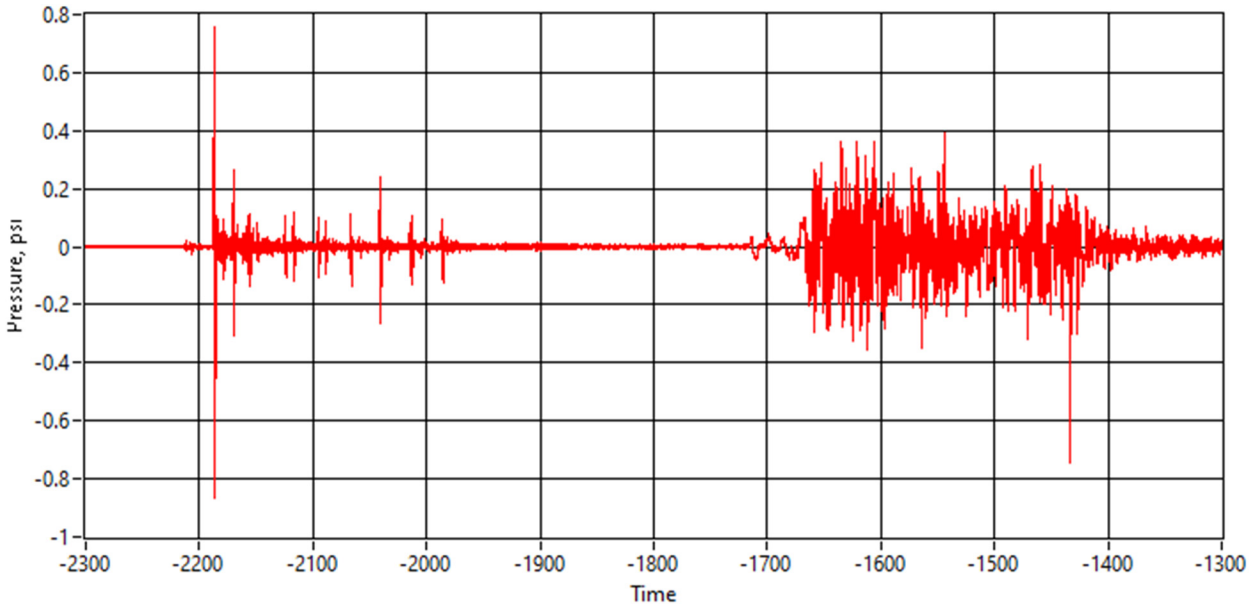

Figure B7: Time history for the hydrophone sensor at WM3 on December 17, 2019

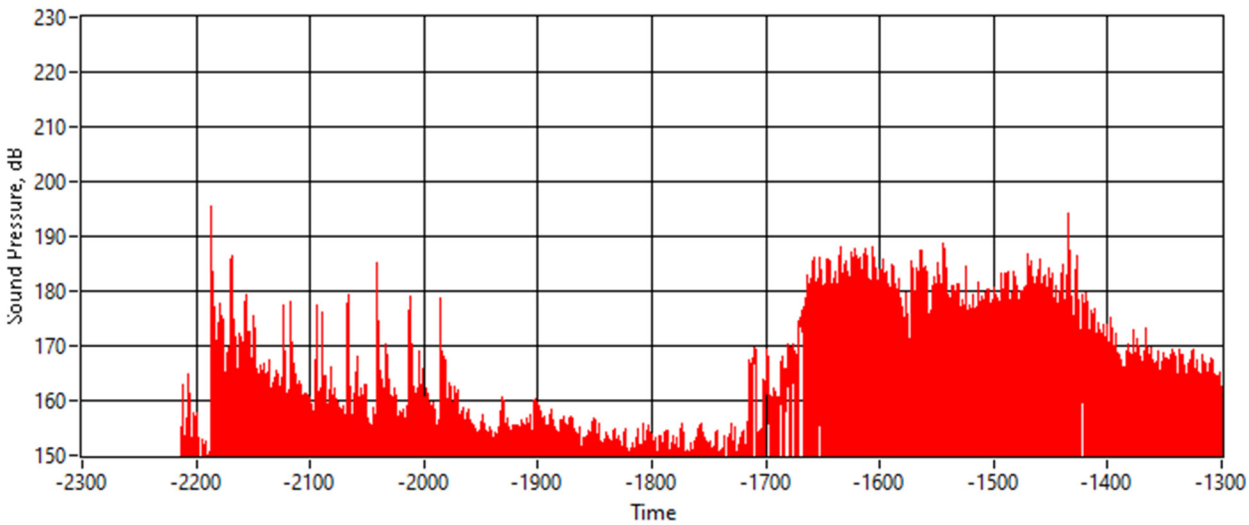

Figure B8: Sound pressure levels for the hydrophone sensor at WM3 on December 17, 2019

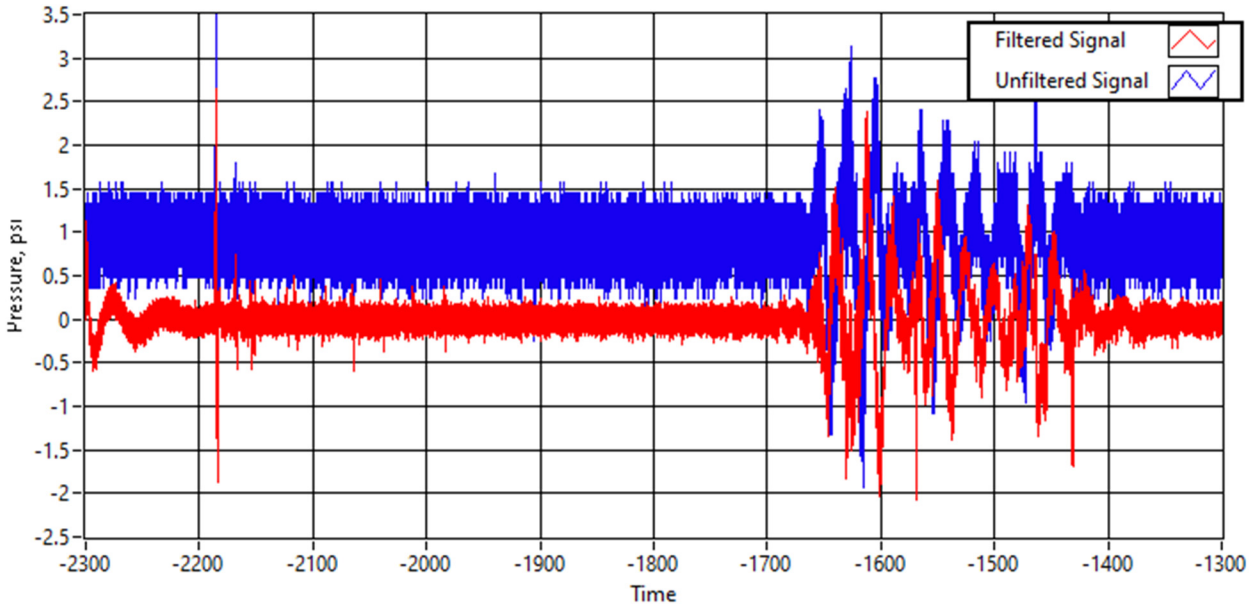

Figure B9: Time history for the PCB sensor at WM4 on December 17, 2019

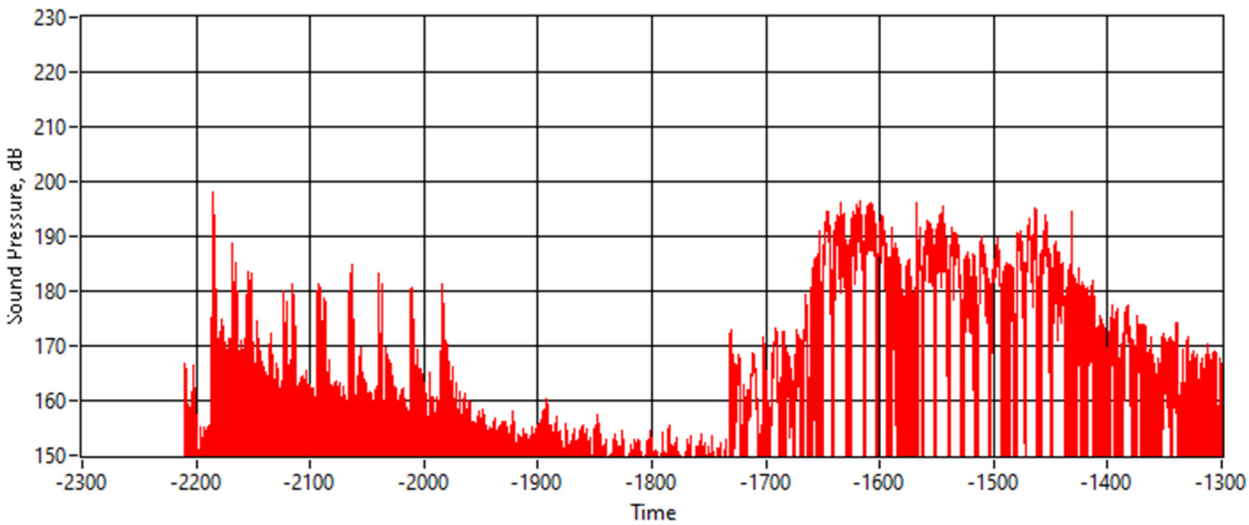

Figure B10: Sound pressure levels for the PCB sensor at WM4 on December 17, 2019 (filtered only)

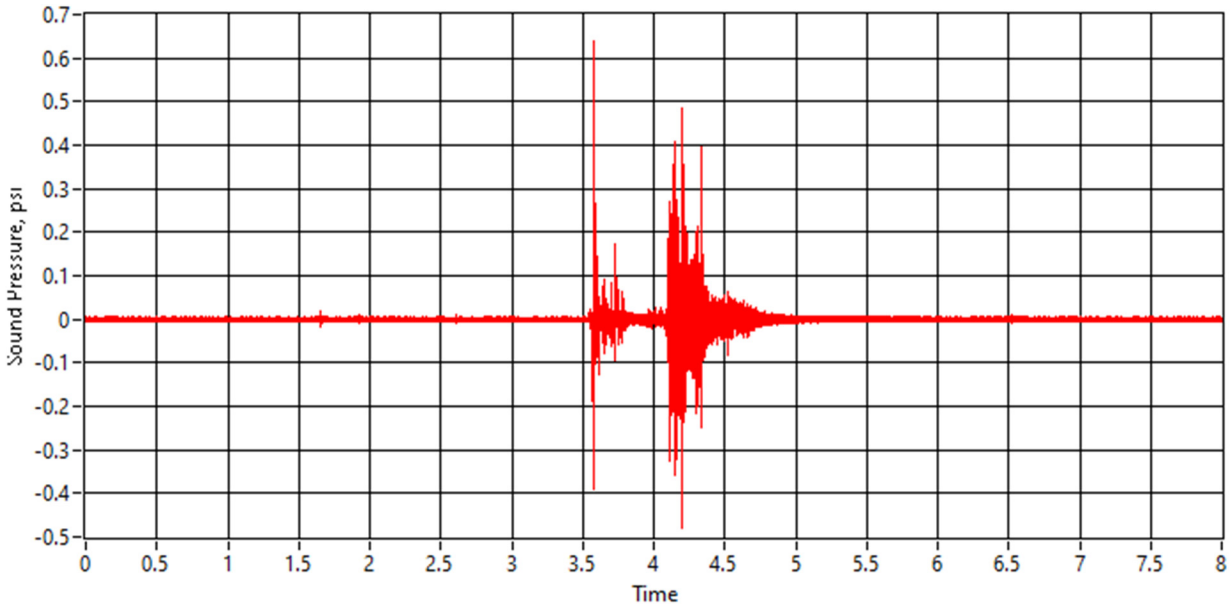

Figure B11: Time history for the hydrophone sensor at WM5 on December 17, 2019

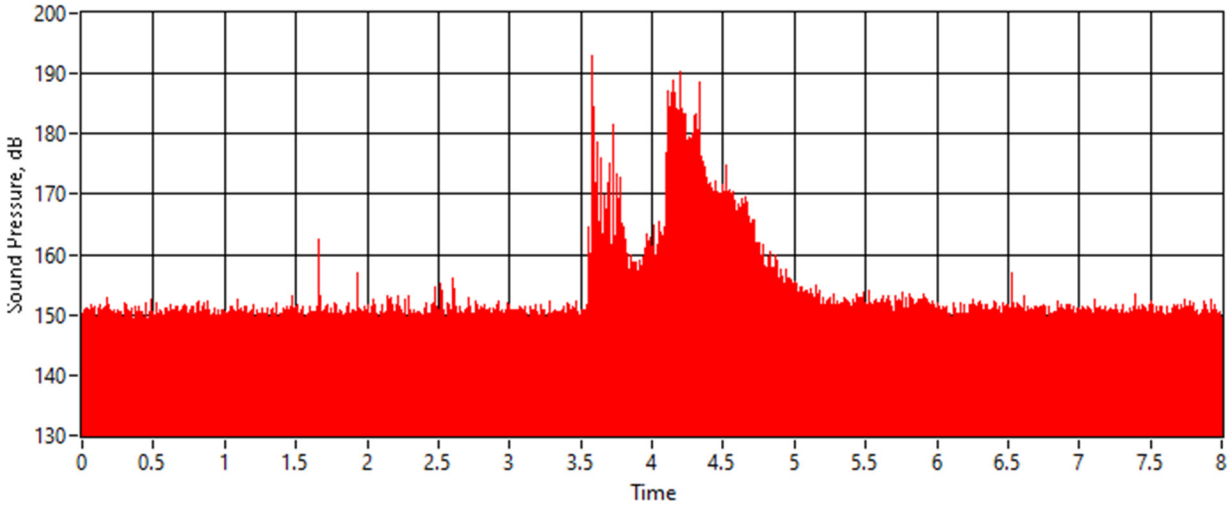

Figure B12: Sound pressure levels for the hydrophone sensor at WM5 on December 17, 2019

December 18, 2019

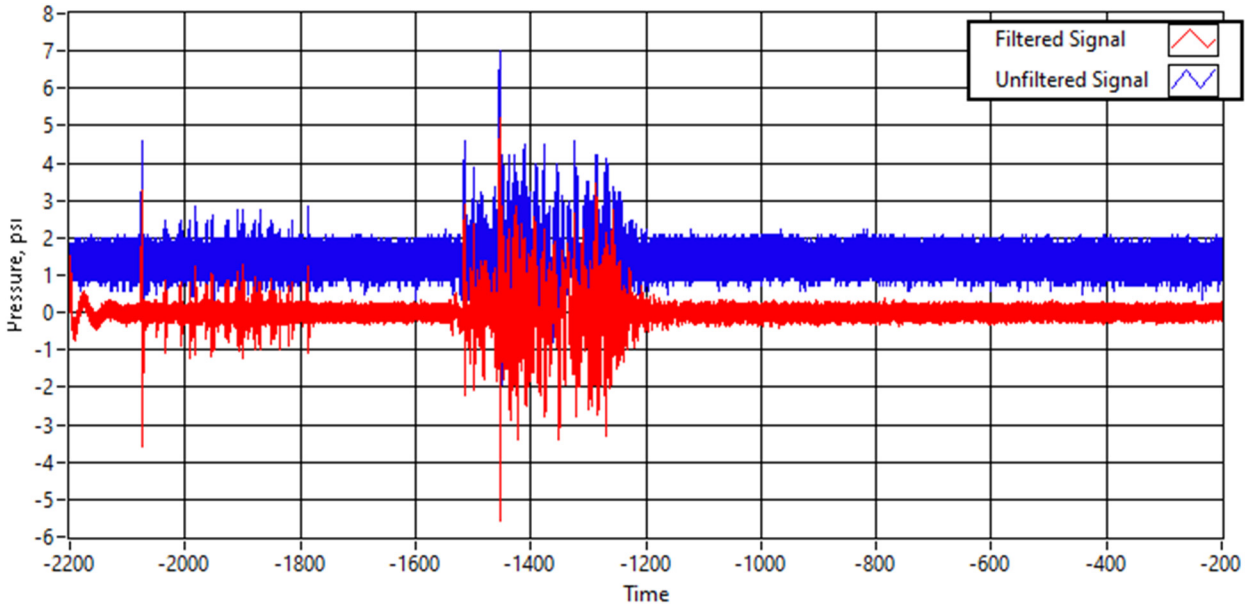

Figure B13: Time history for the PCB sensor at WM1 on December 18, 2019

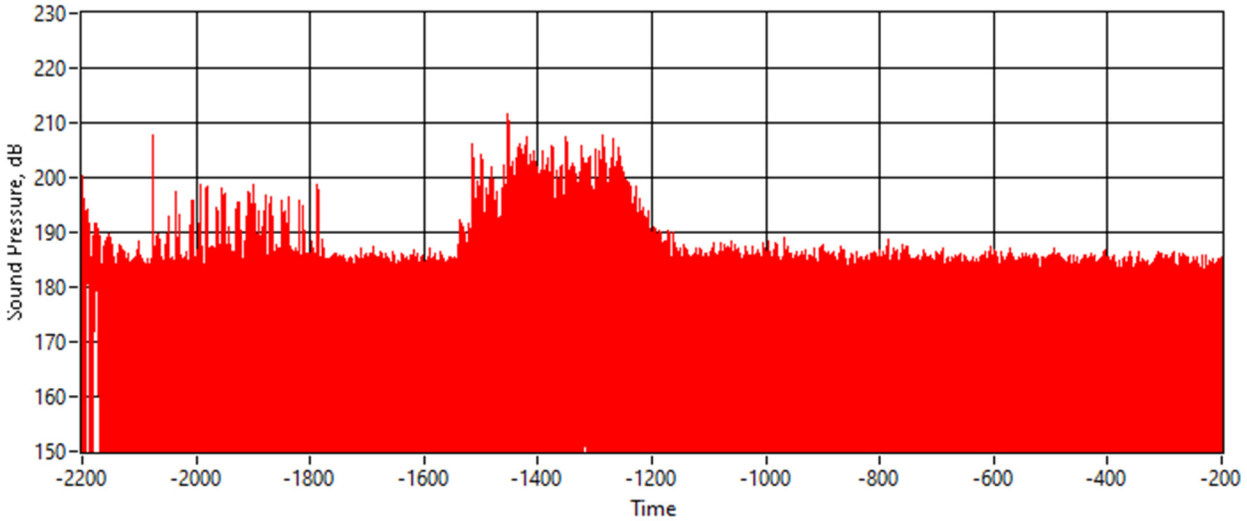

Figure B14: Sound pressure levels for the PCB sensor at WM1 on December 18, 2019 (filtered only)

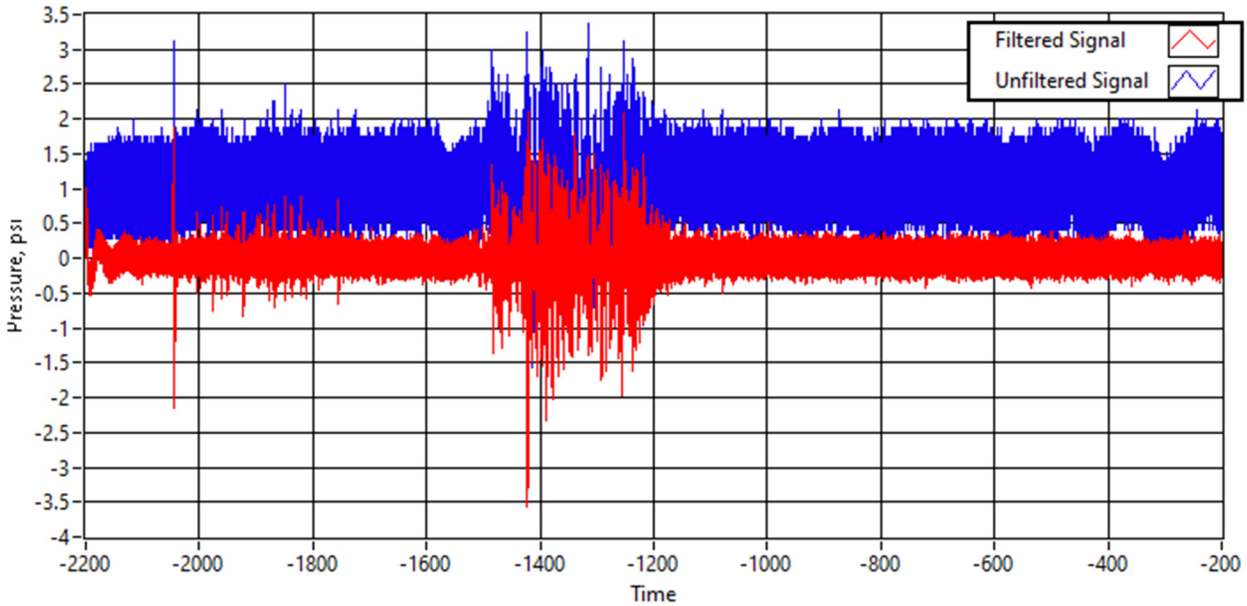

Figure B15: Time history for the PCB sensor at WM2 on December 18, 2019

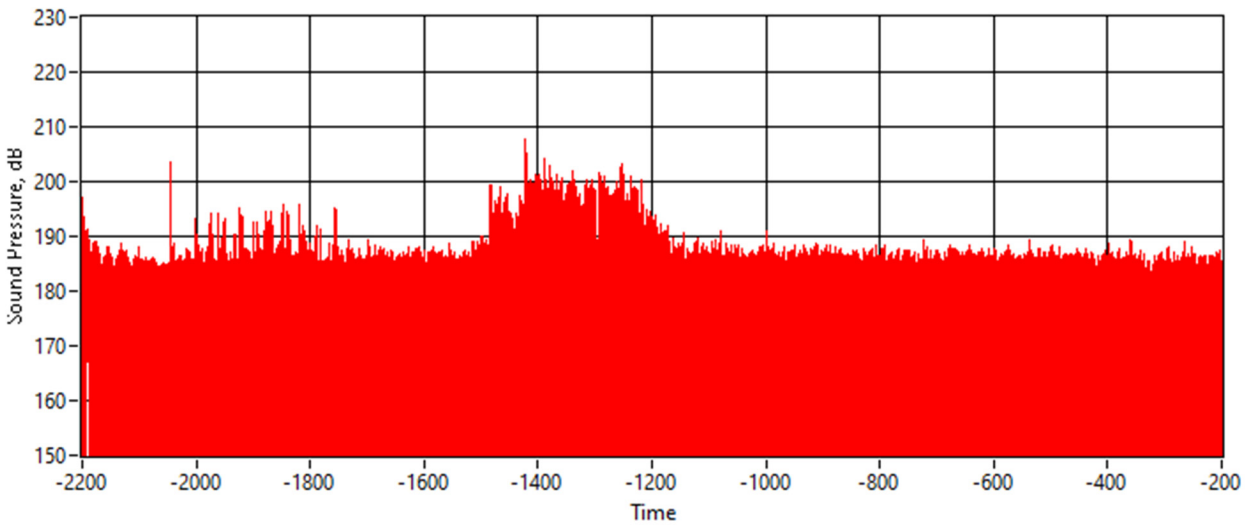

Figure B16: Sound pressure levels for the PCB sensor at WM2 on December 18, 2019 (filtered only)

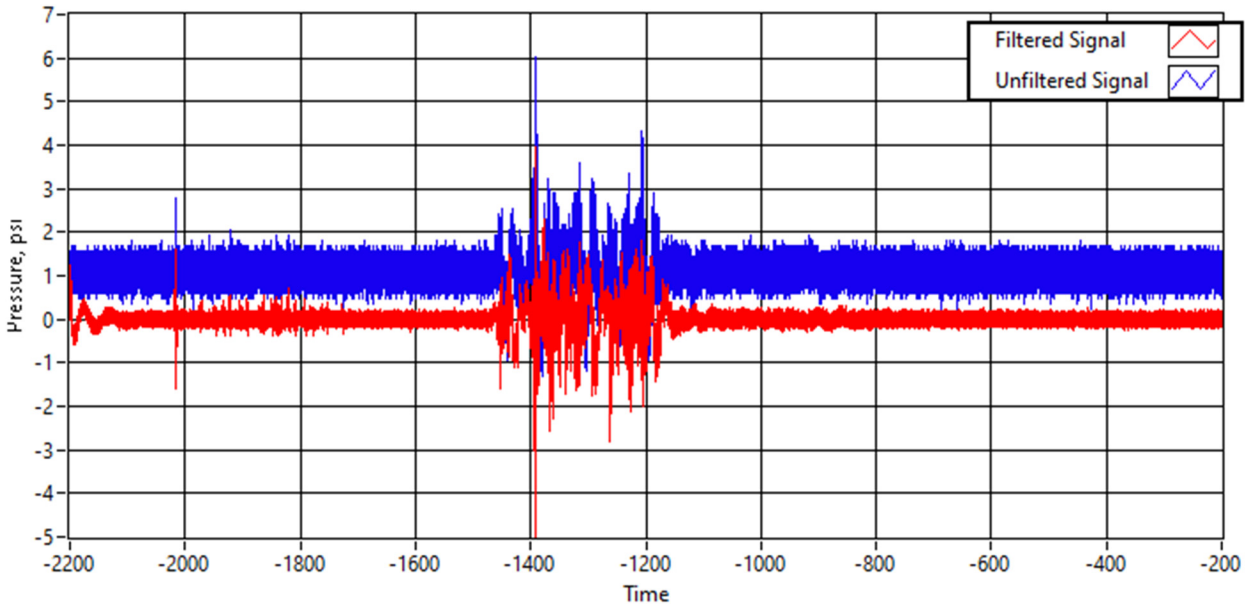

Figure B17: Time history for the PCB sensor at WM3 on December 18, 2019

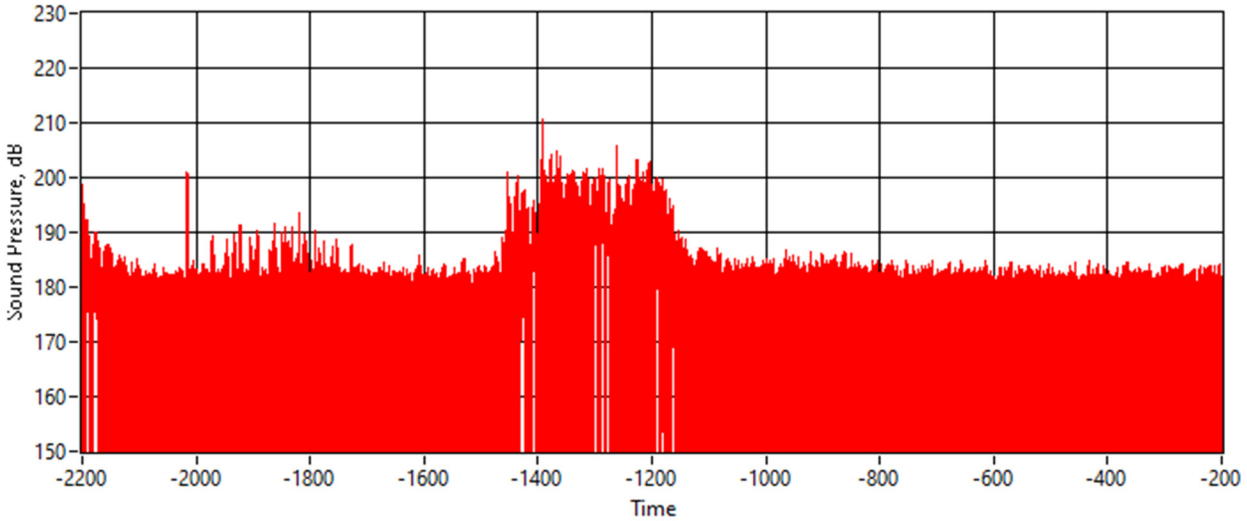

Figure B18: Sound pressure levels for the PCB sensor at WM3 on December 18, 2019 (filtered only)

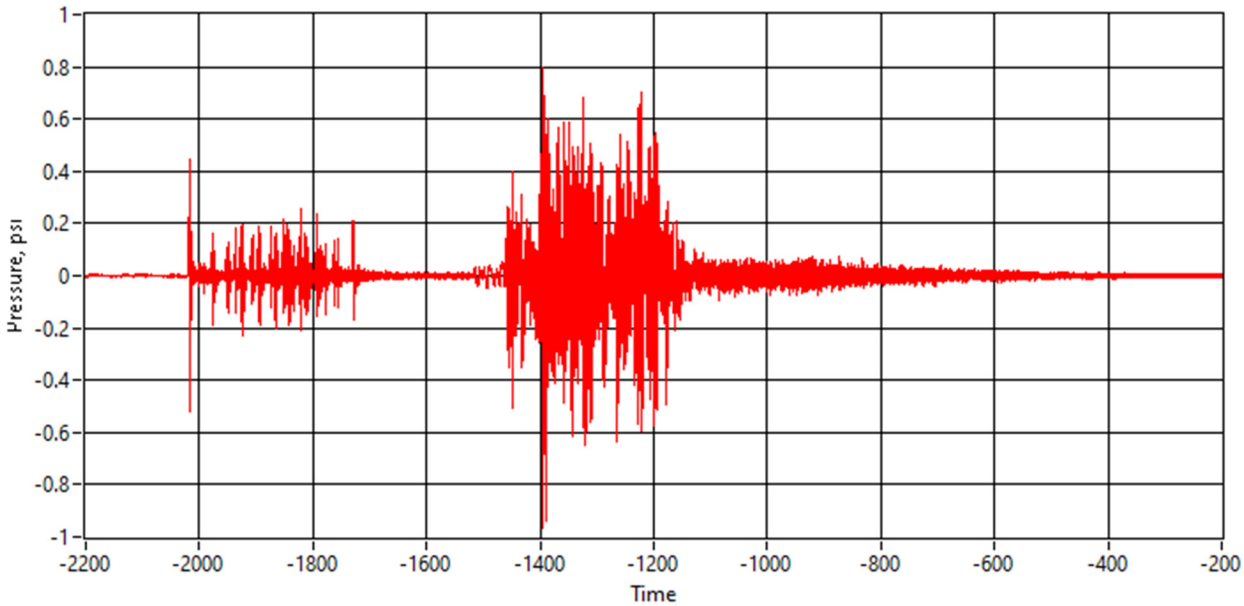

Figure B19: Time history for the hydrophone sensor at WM3 on December 18, 2019

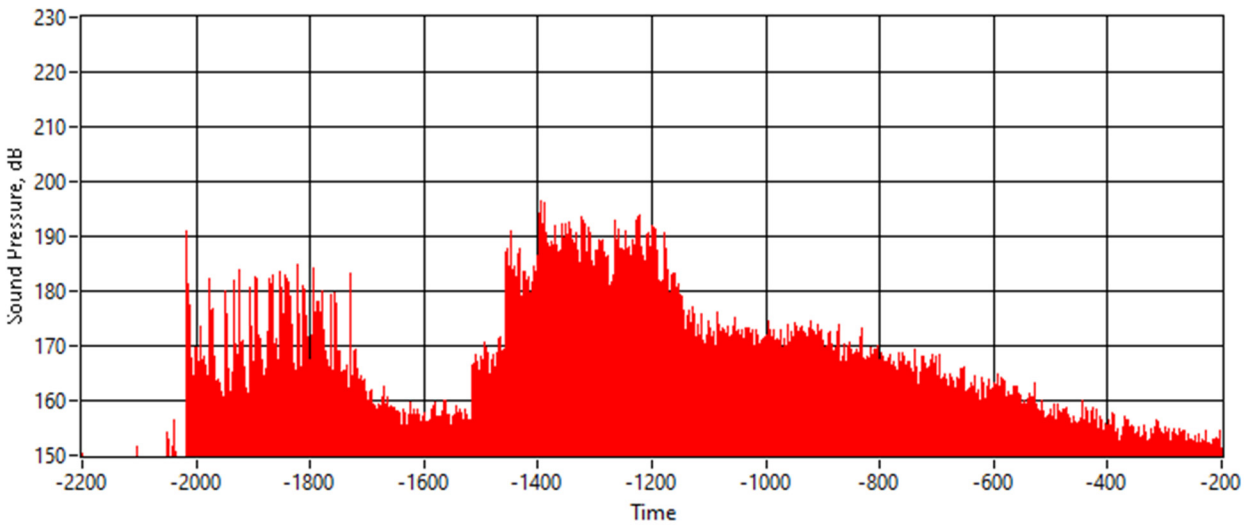

Figure B20: Sound pressure levels for the hydrophone sensor at WM3 on December 18, 2019

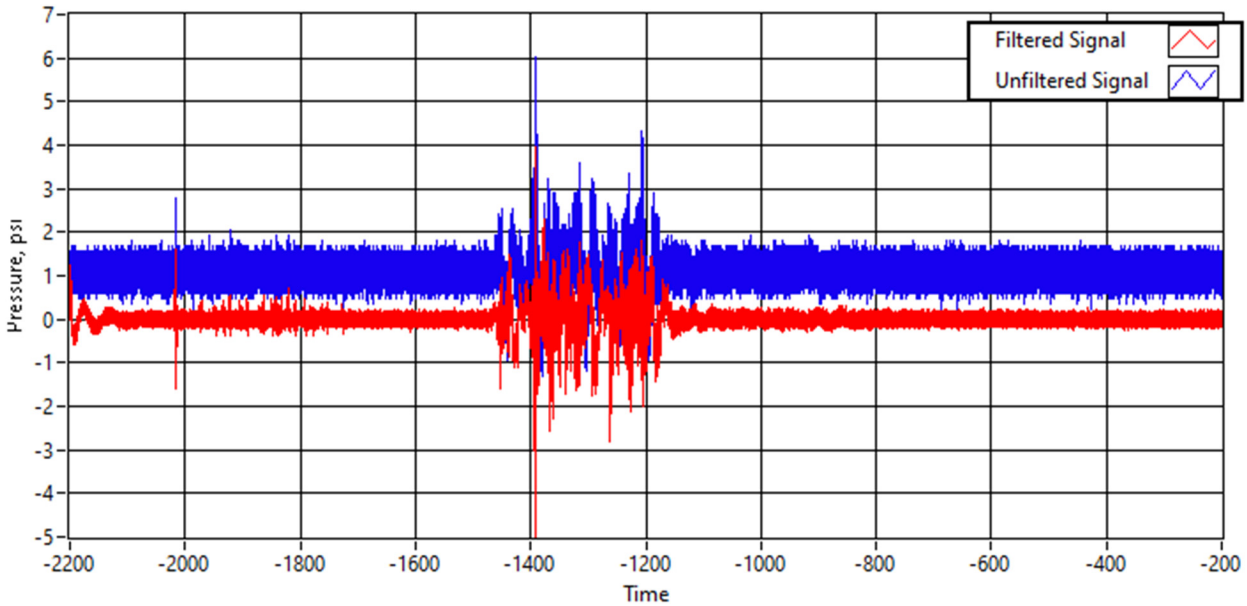

Figure B21: Time history for the PCB sensor at WM4 on December 18, 2019

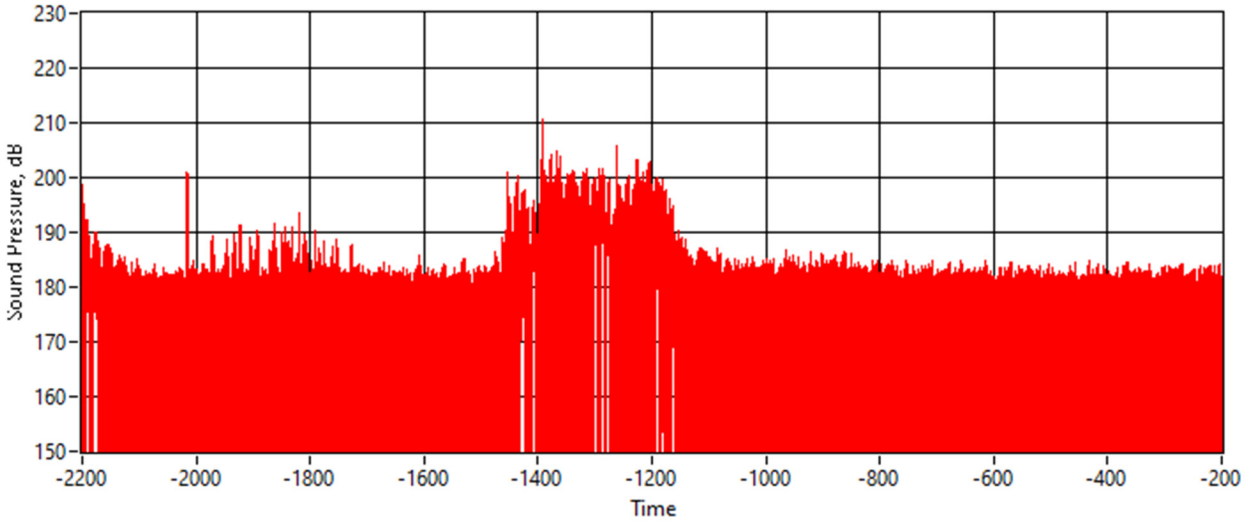

Figure B22: Sound pressure levels for the PCB sensor at WM4 on December 18, 2019 (filtered only)

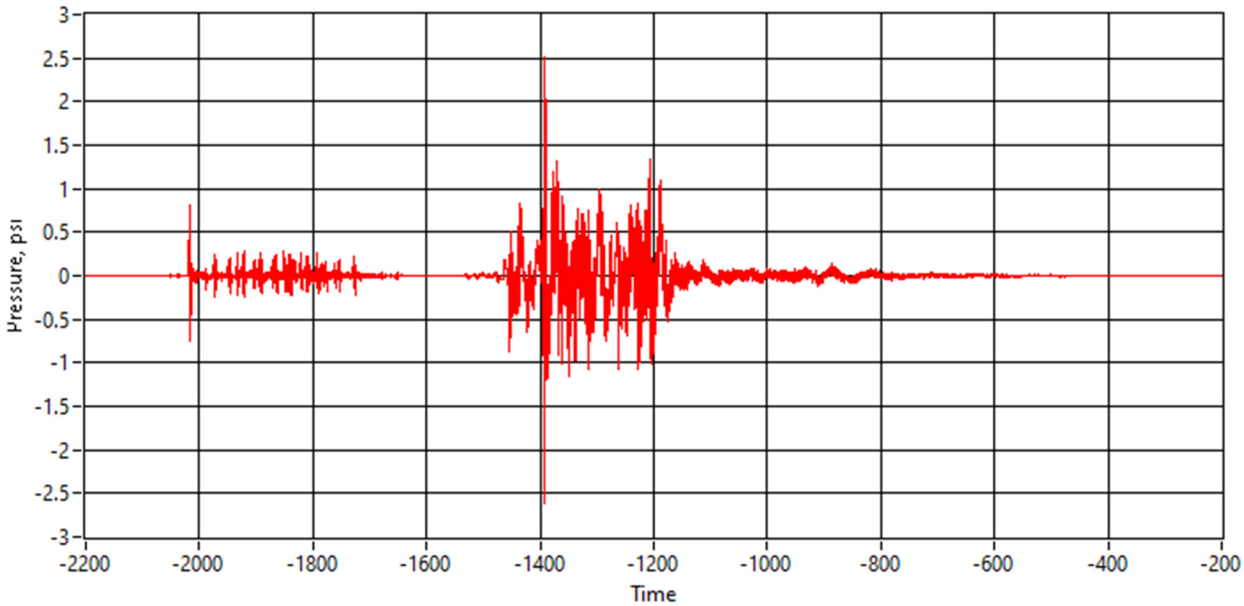

Figure B23: Time history for the hydrophone sensor at WM4 on December 18, 2019

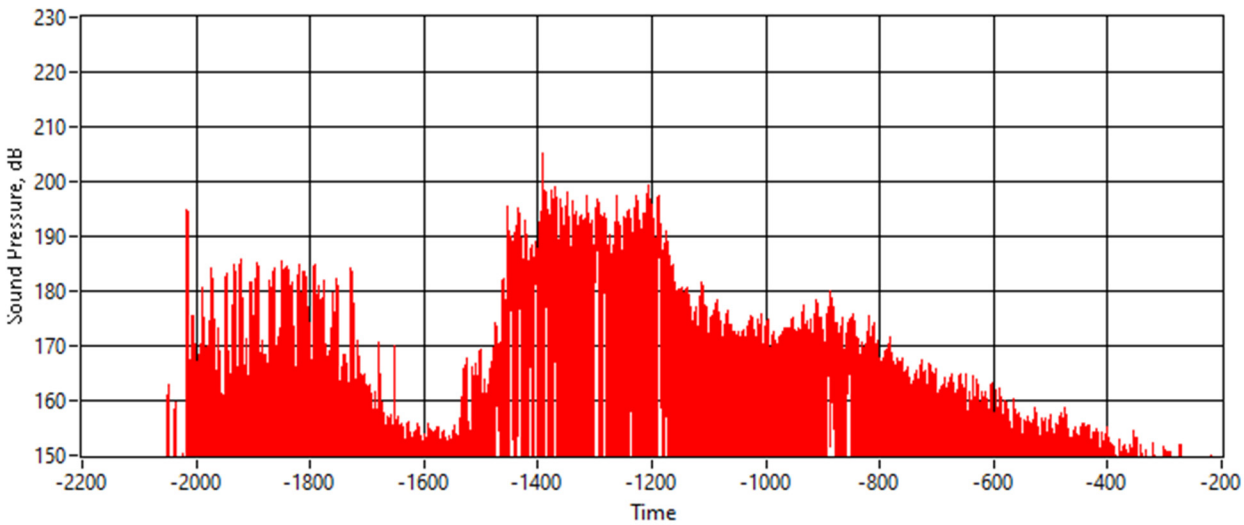

Figure B24: Sound pressure levels for the hydrophone sensor at WM4 on December 18, 2019

December 19, 2019

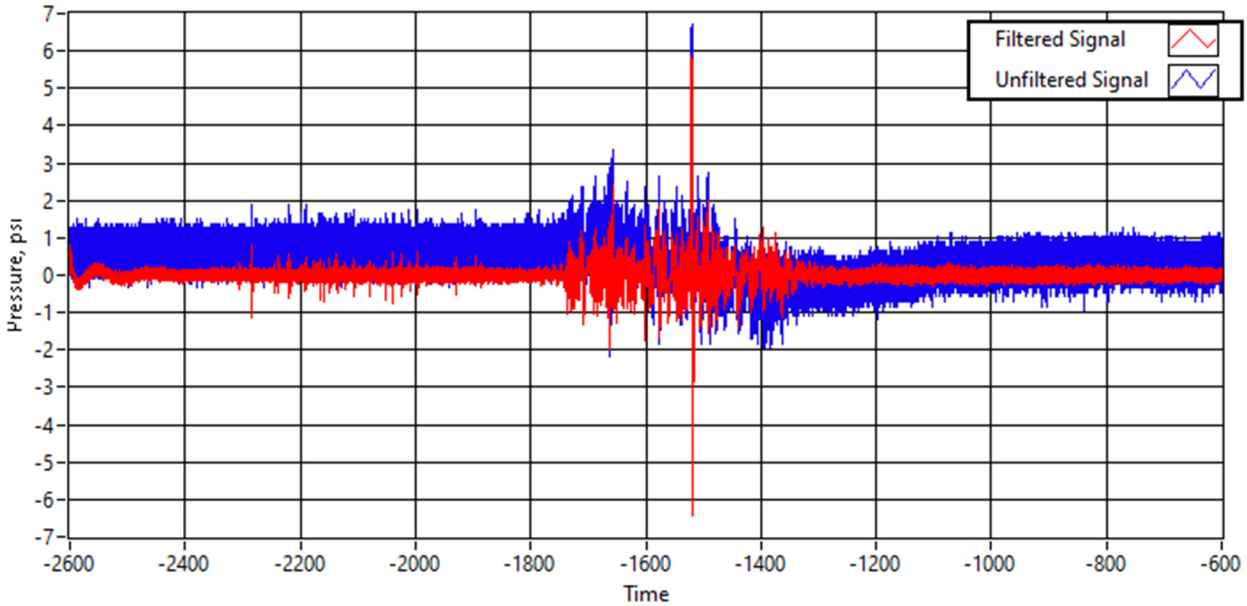

Figure B25: Time history for the PCB sensor at WM2 on December 19, 2019

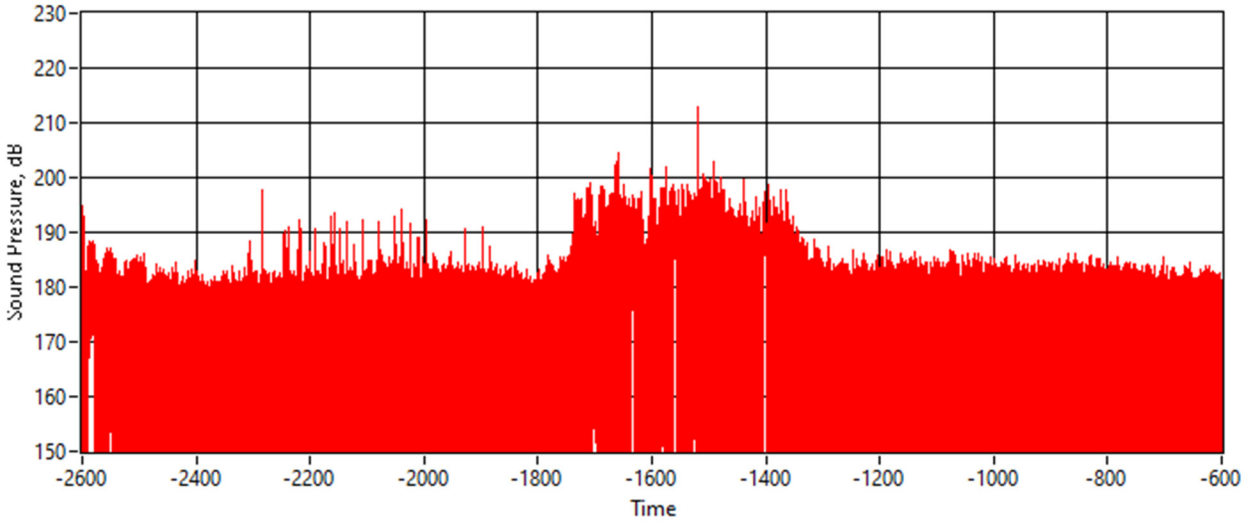

Figure B26: Sound pressure levels for the PCB sensor at WM2 on December 19, 2019 (filtered only)

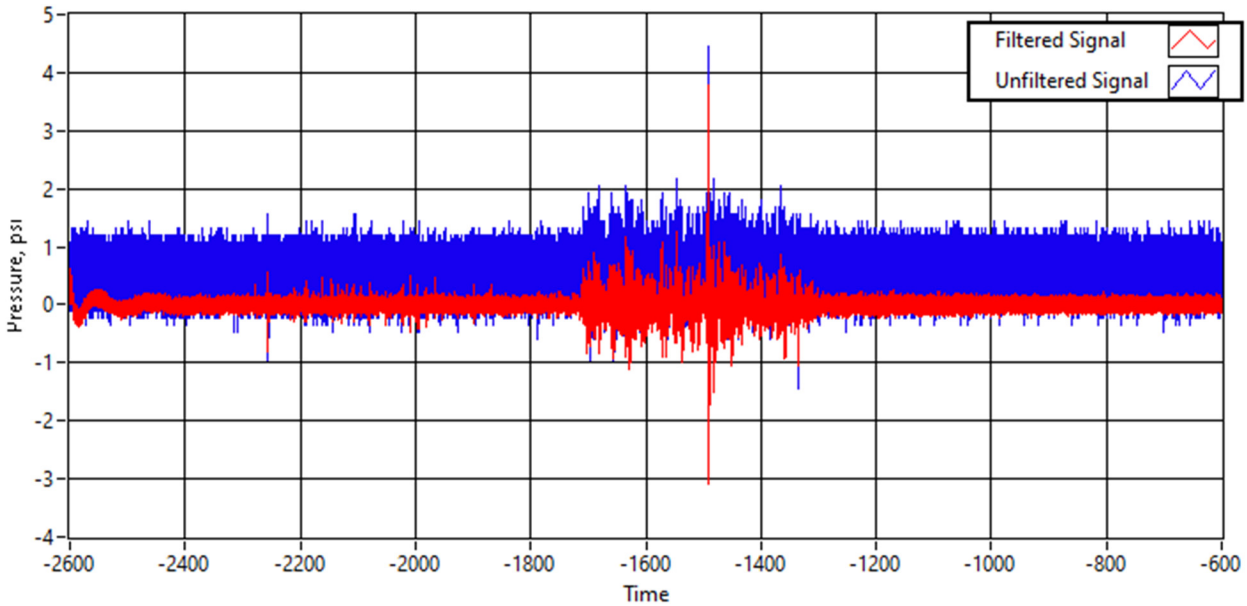

Figure B27: Time history for the PCB sensor at WM3 on December 19, 2019

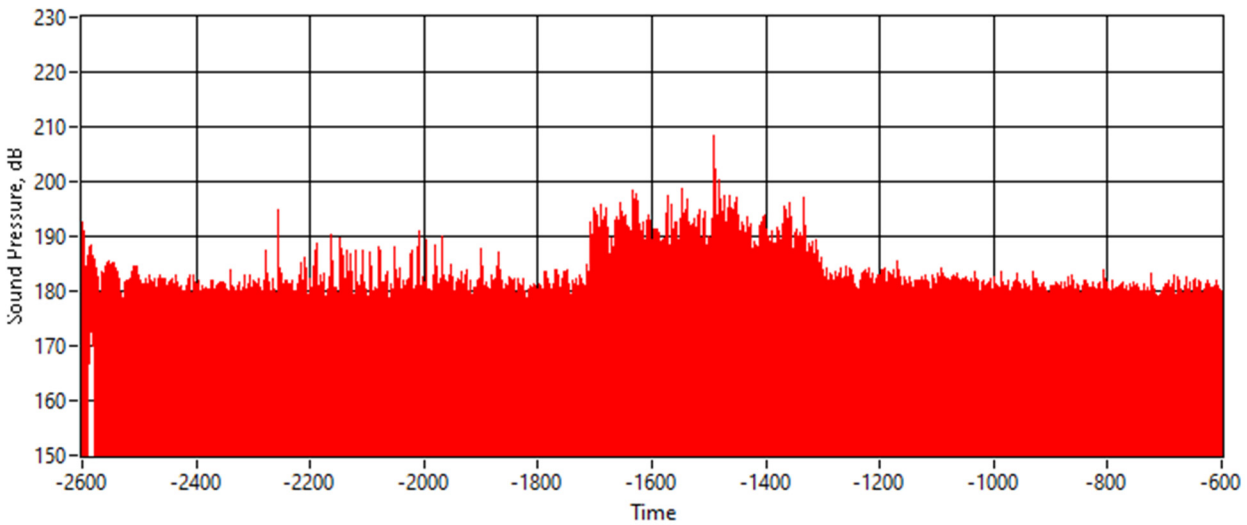

Figure B28: Sound pressure levels for the PCB sensor at WM3 on December 19, 2019 (filtered only)

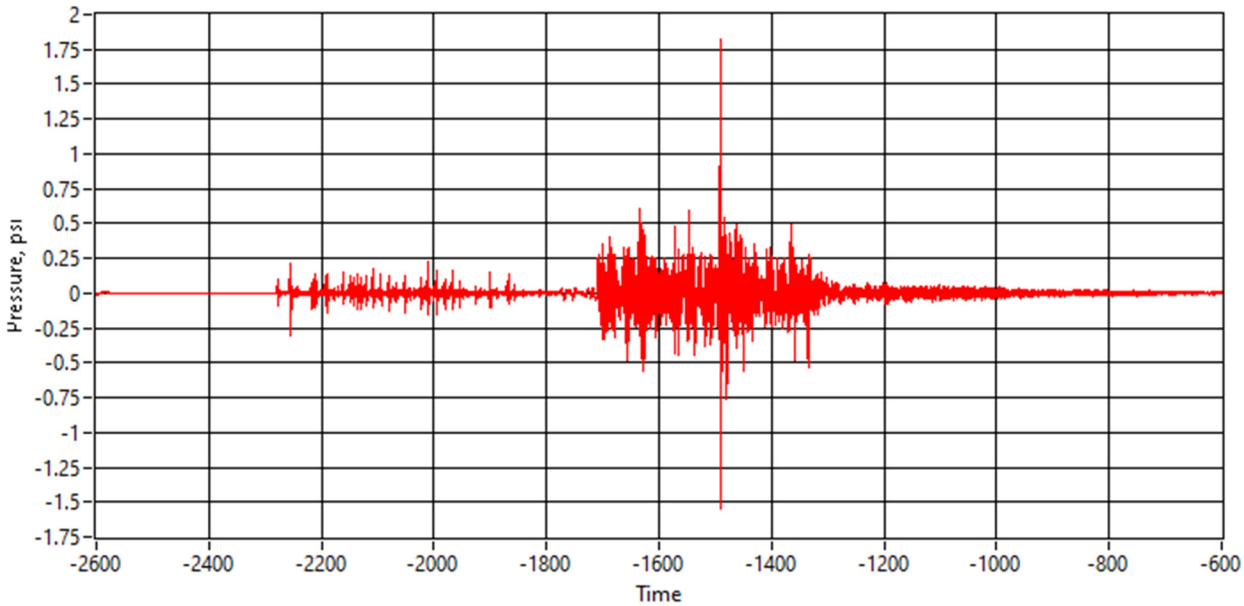

Figure B29: Time history for the hydrophone sensor at WM3 on December 19, 2019

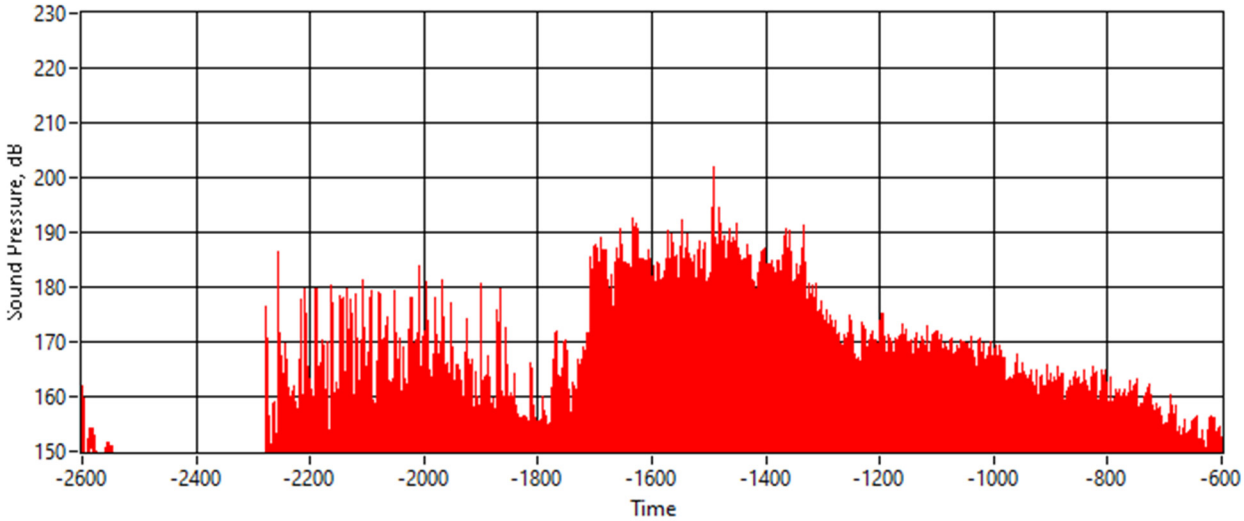

Figure B30: Sound pressure levels for the hydrophone sensor at WM3 on December 19, 2019

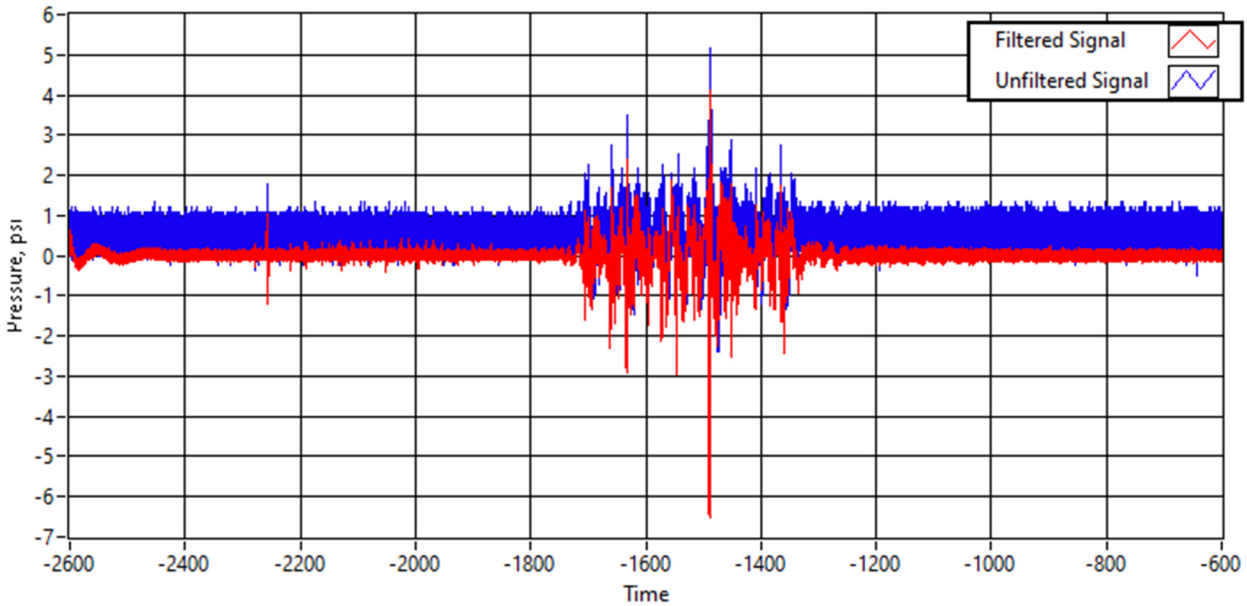

Figure B31: Time history for the PCB sensor at WM4 on December 19, 2019

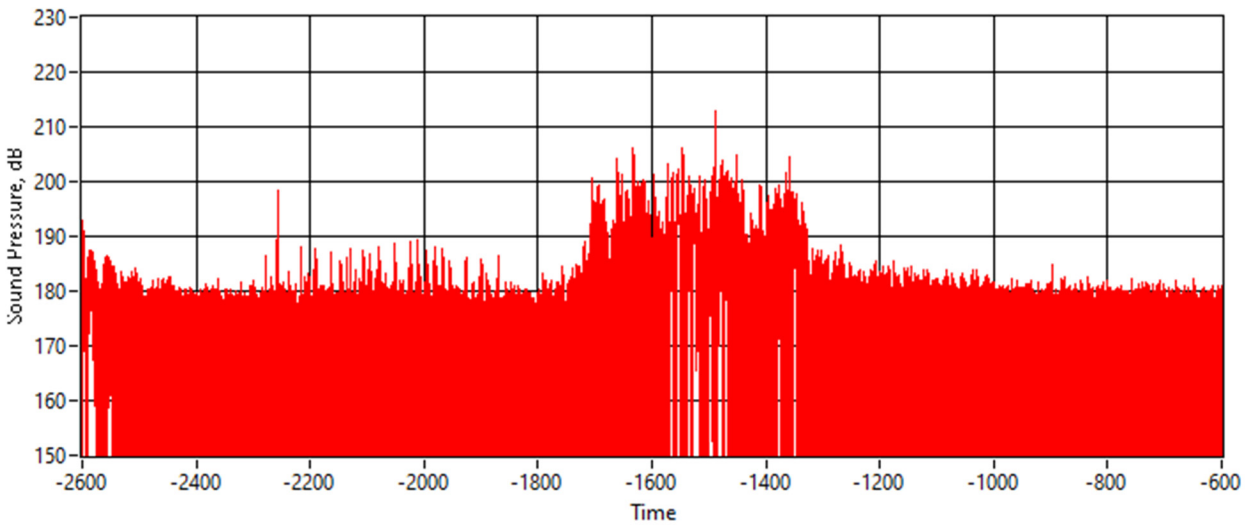

Figure B32: Sound pressure levels for the PCB sensor at WM4 on December 19, 2019 (filtered only)

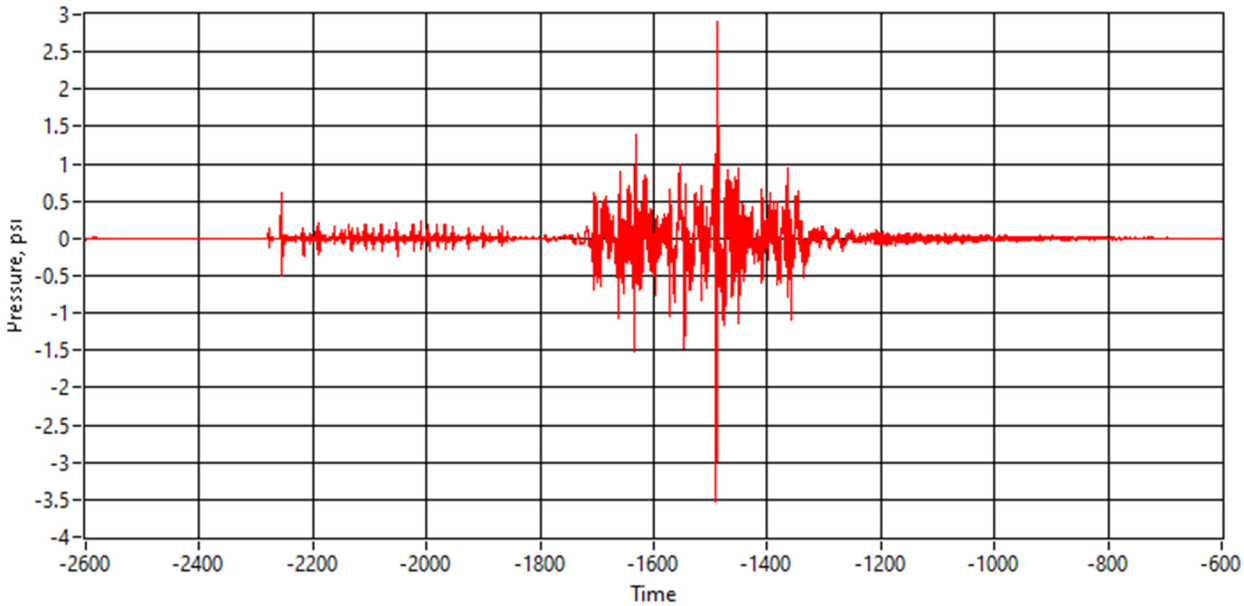

Figure B33: Time history for the hydrophone sensor at WM4 on December 19, 2019

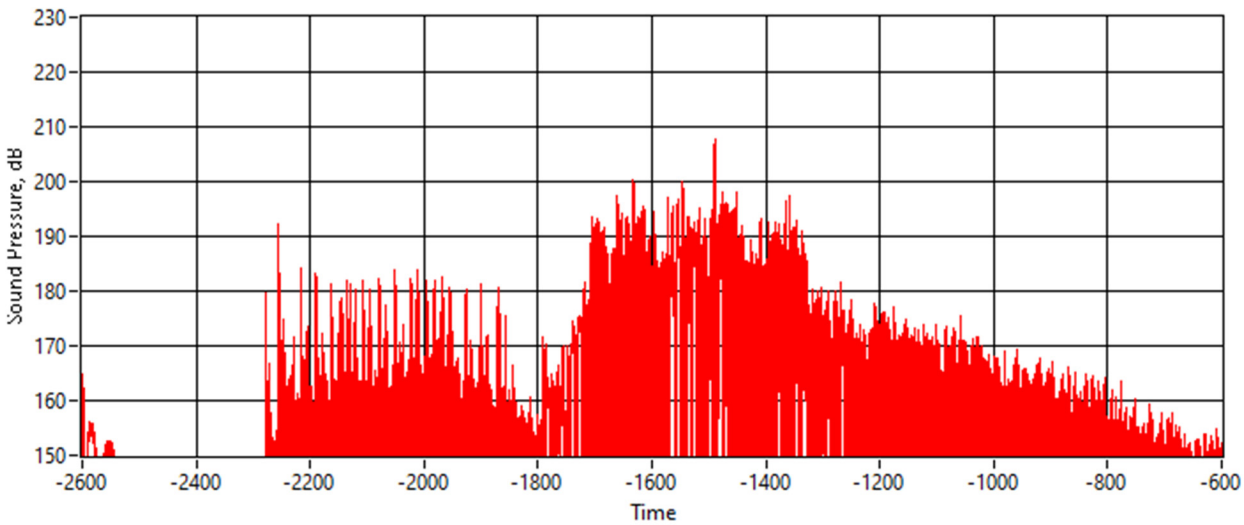

Figure B34: Sound pressure levels for the hydrophone sensor at WM4 on December 19, 2019

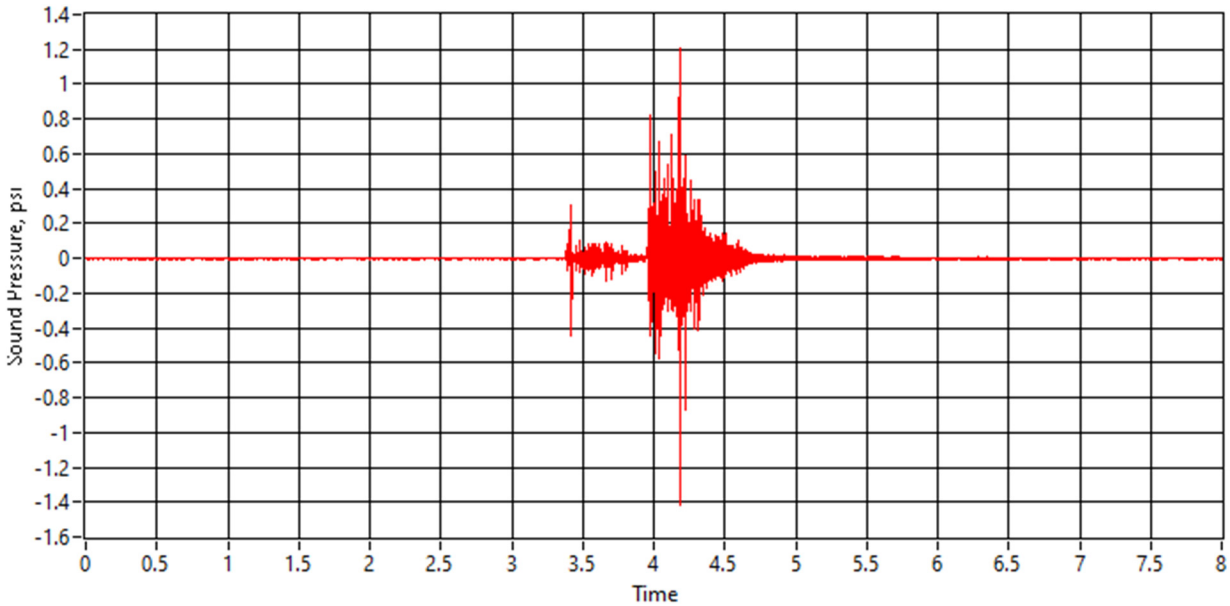

Figure B35: Time history for the hydrophone sensor at WM5a on December 19, 2019

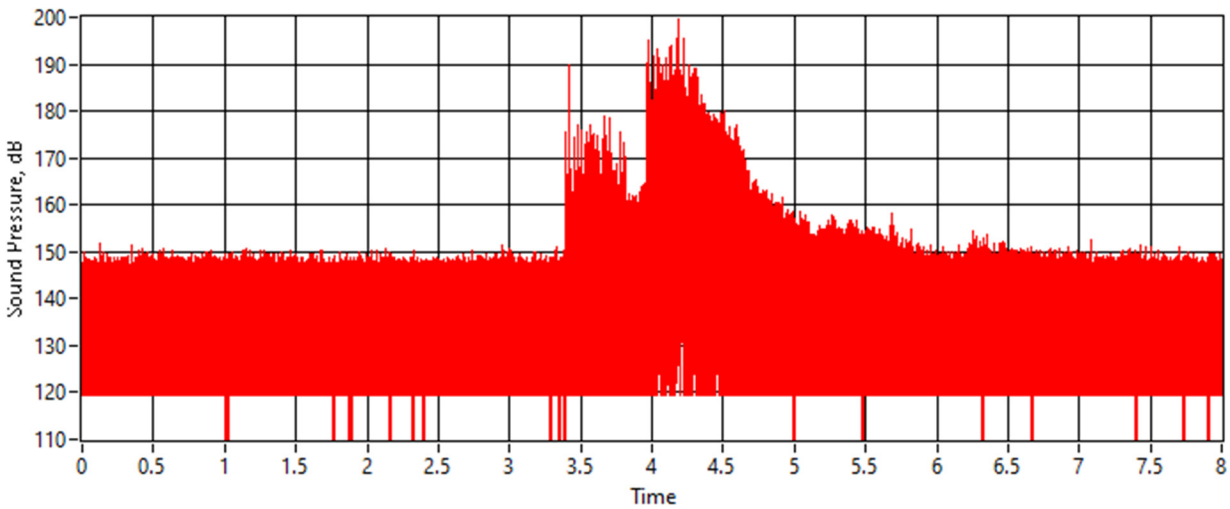

Figure B36: Sound pressure levels for the hydrophone sensor at WM5a on December 19, 2019

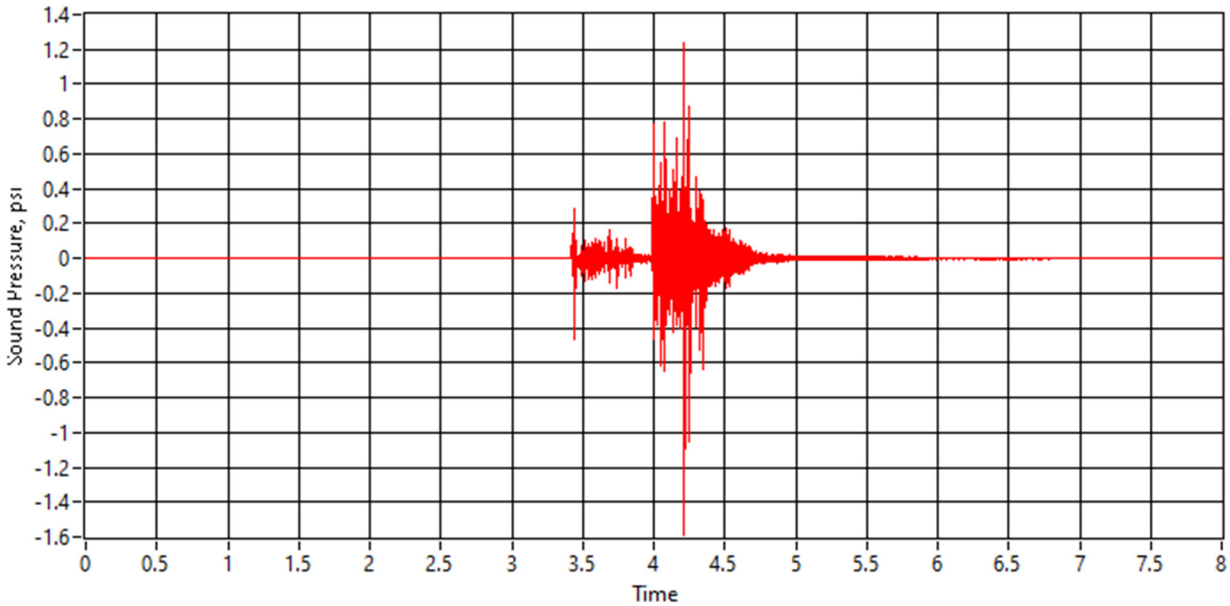

Figure B37: Time history for the hydrophone sensor at WM5b on December 19, 2019

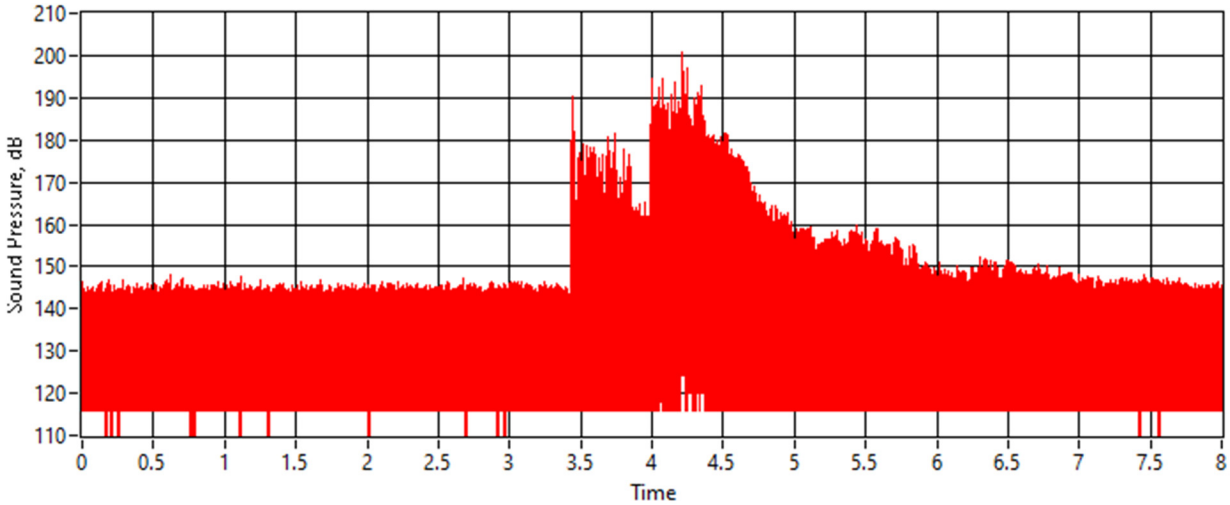

Figure B38: Sound pressure levels for the hydrophone sensor at WM5b on December 19, 2019

December 20, 2019

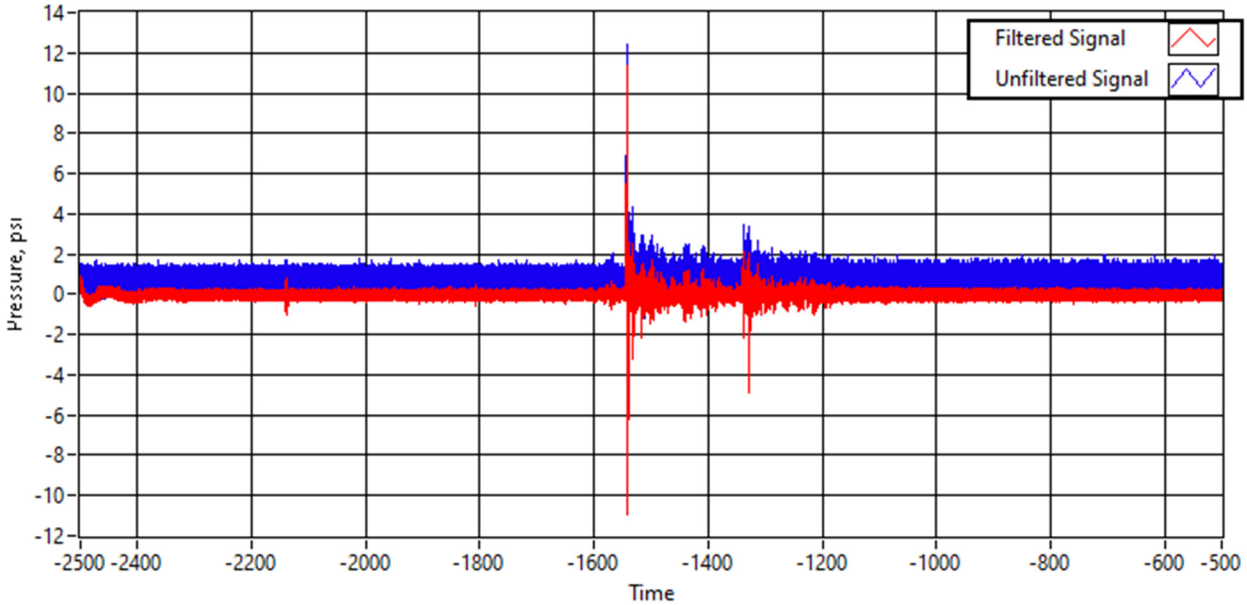

Figure B39: Time history for the PCB sensor at WM3 on December 20, 2019

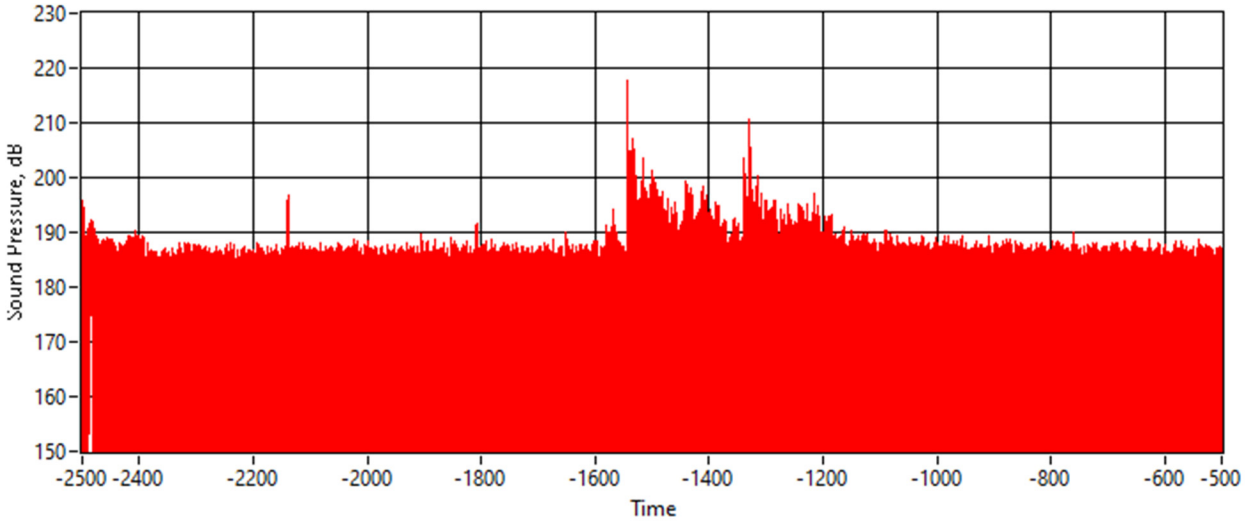

Figure B40: Sound pressure levels for the PCB sensor at WM3 on December 20, 2019 (filtered only)

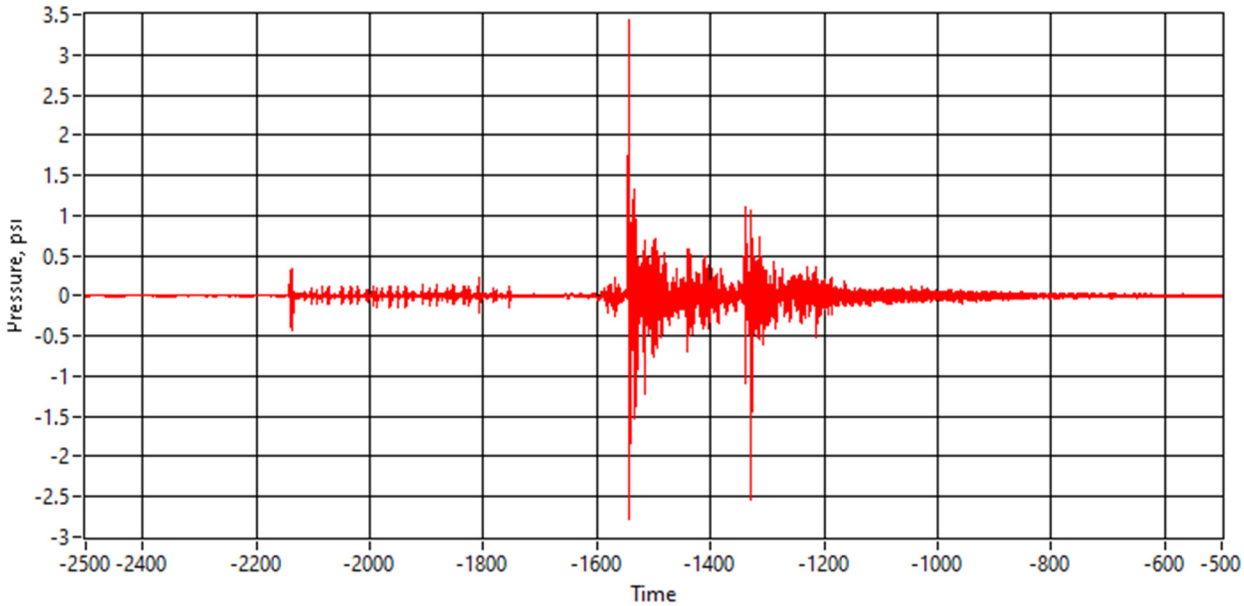

Figure B41: Time history for the hydrophone sensor at WM3 on December 20, 2019

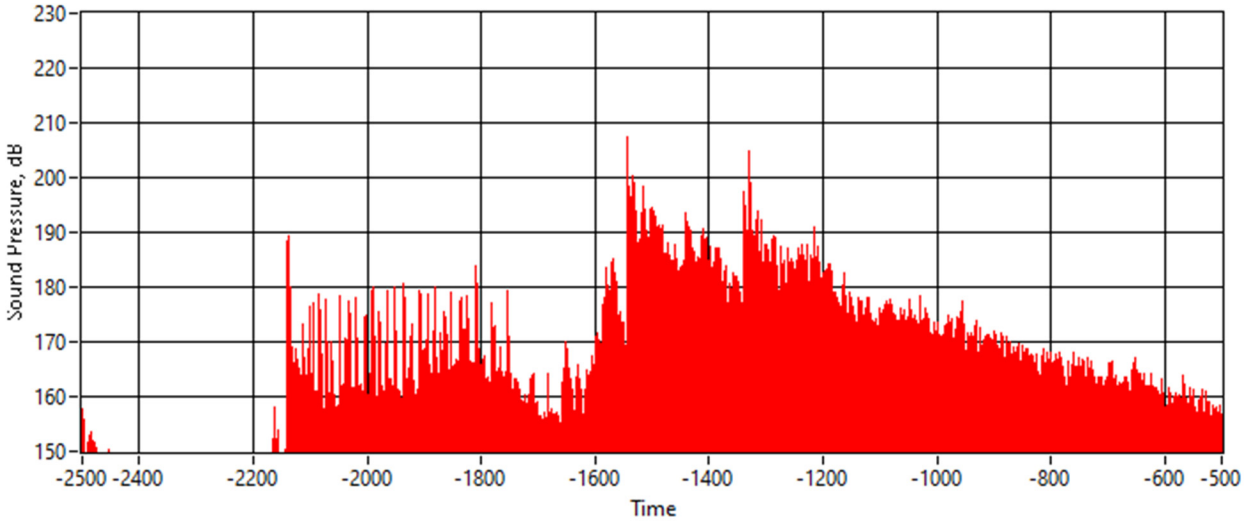

Figure B42: Sound pressure levels for the hydrophone sensor at WM3 on December 20, 2019

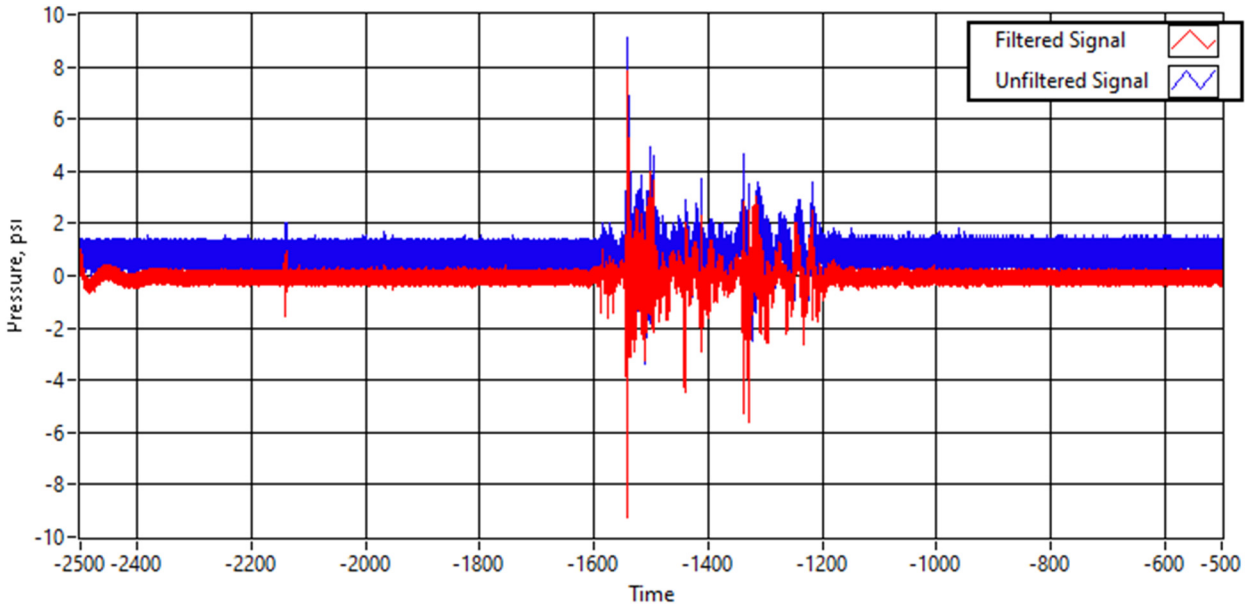

Figure B43: Time history for the PCB sensor at WM4 on December 20, 2019

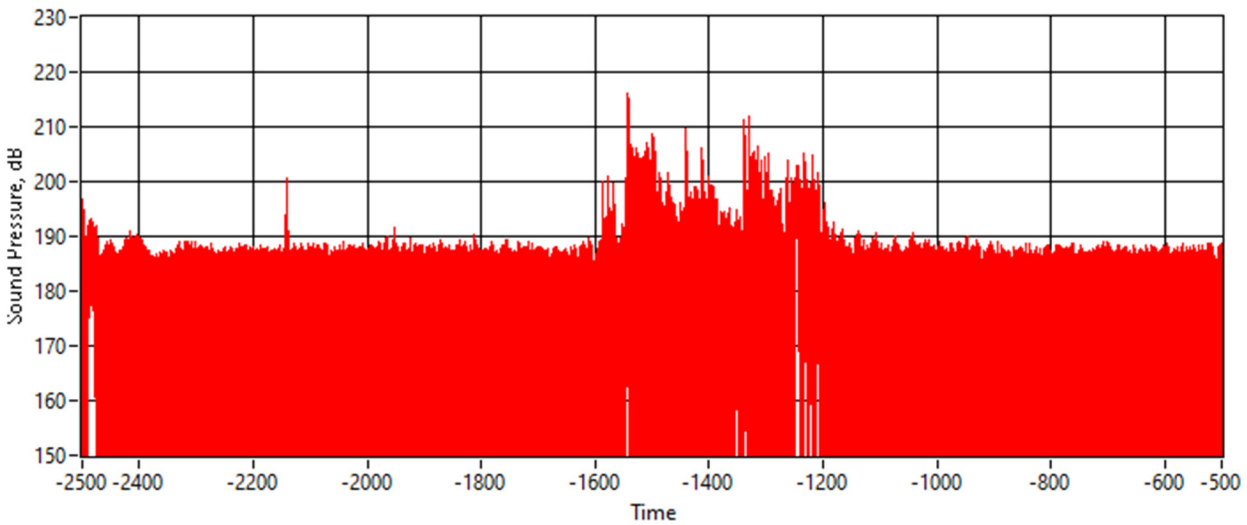

Figure B44: Sound pressure levels for the PCB sensor at WM4 on December 20, 2019 (filtered only)

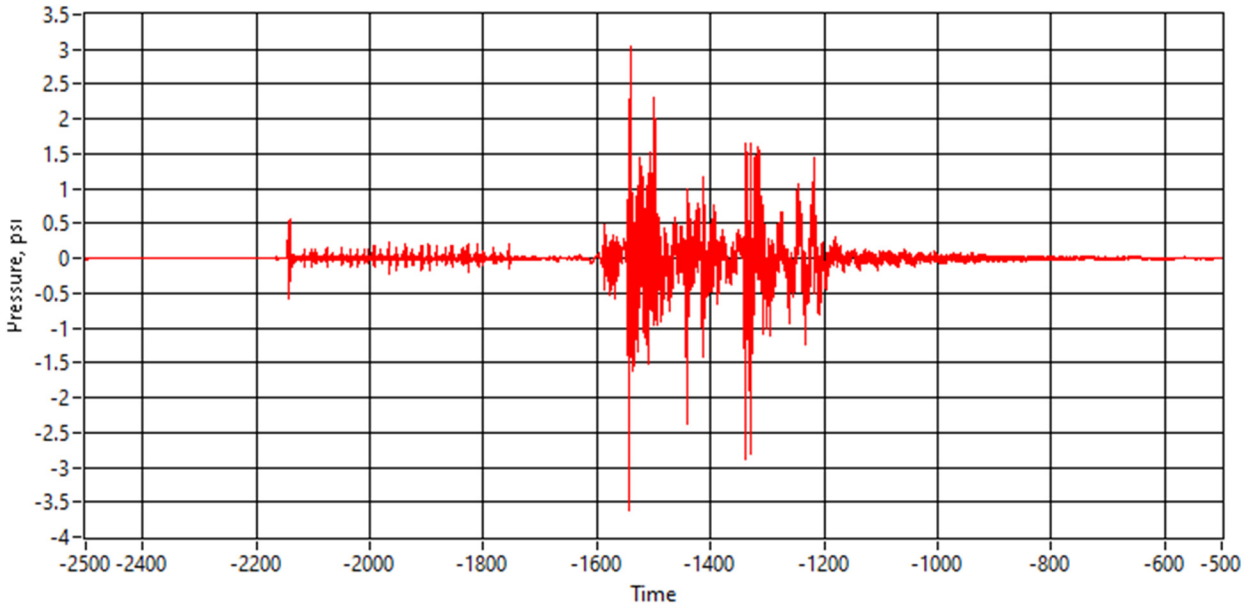

Figure B45: Time history for the hydrophone sensor at WM4 on December 20, 2019

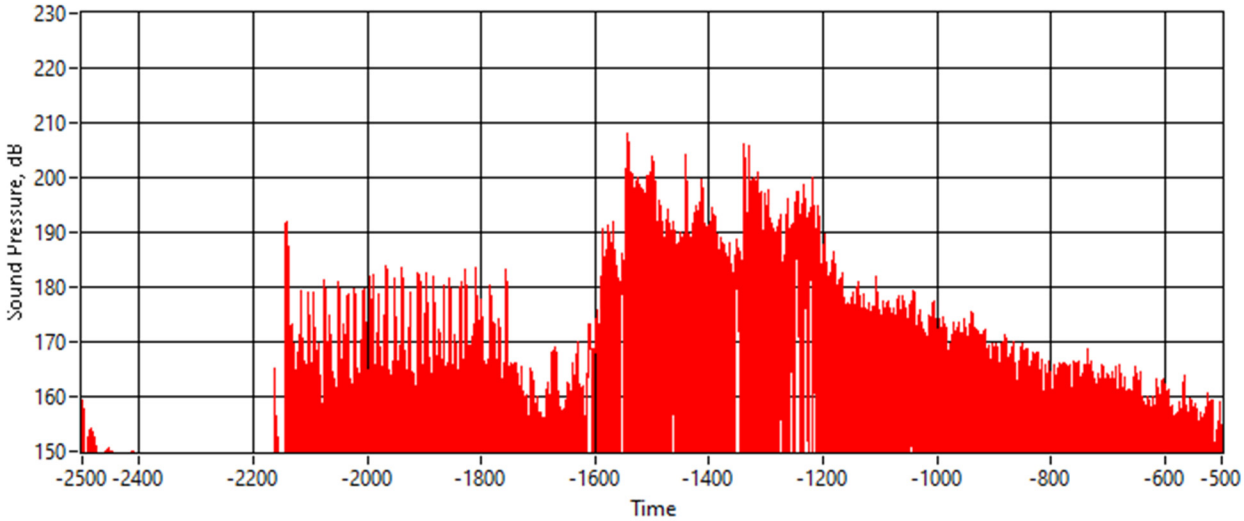

Figure B46: Sound pressure levels for the hydrophone sensor at WM4 on December 20, 2019

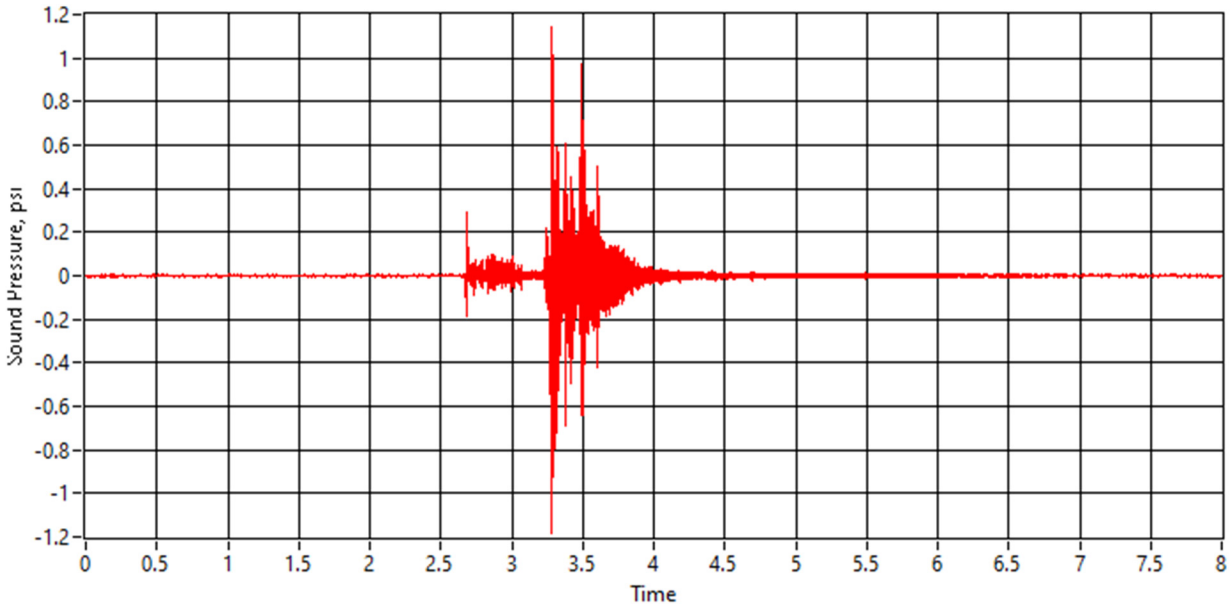

Figure B47: Time history for the hydrophone sensor at WM5 on December 20, 2019

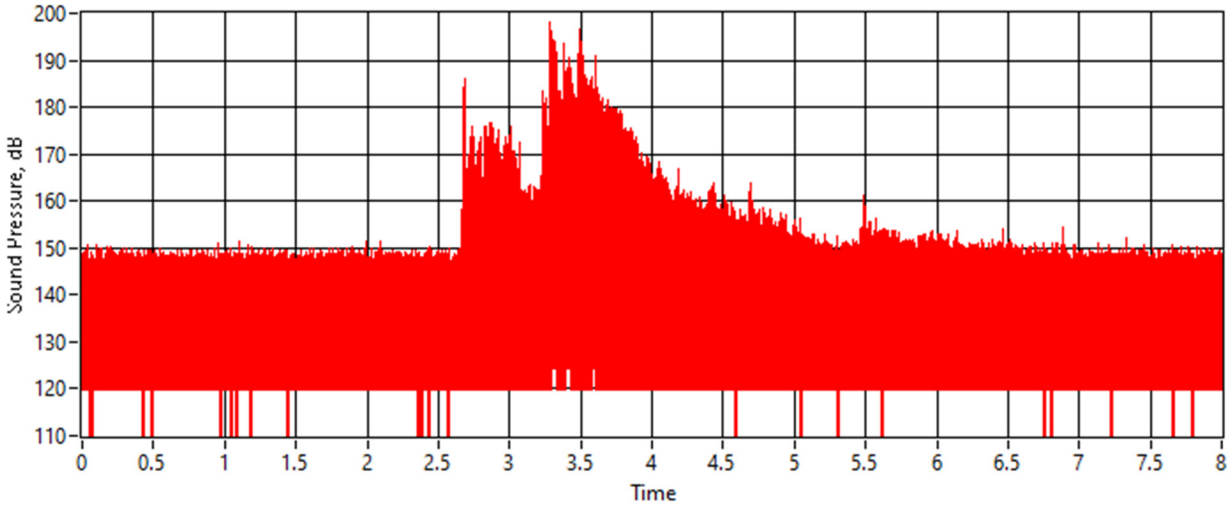

Figure B48: Sound pressure levels for the hydrophone sensor at WM5 on December 20, 2019

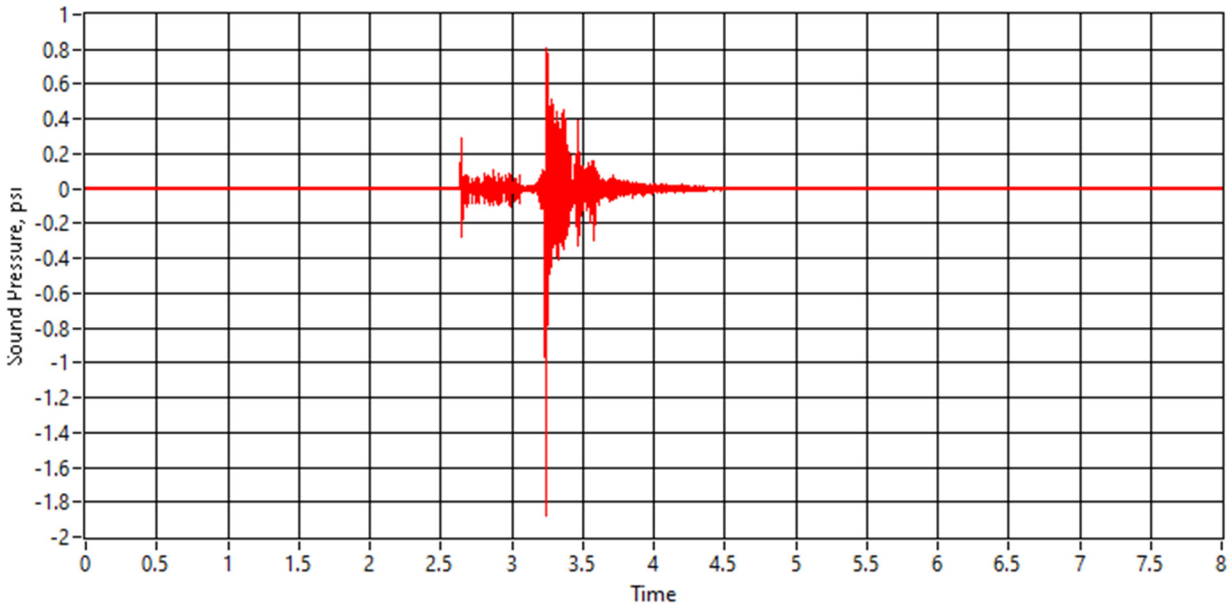

Figure B49: Time history for the hydrophone sensor at WM6 on December 20, 2019

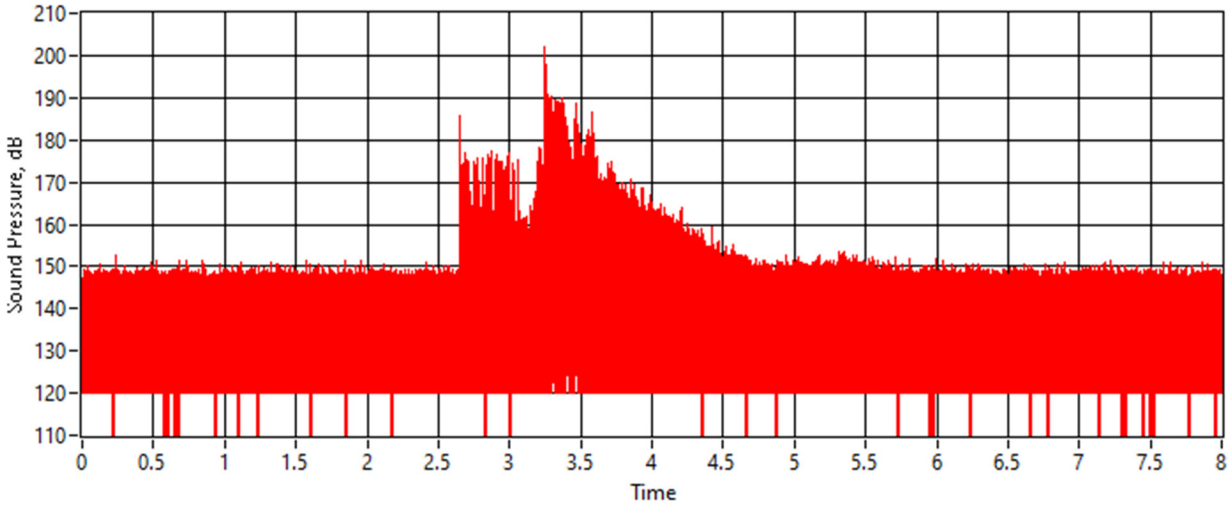

Figure B50: Sound pressure levels for the hydrophone sensor at WM6 on December 20, 2019

APPENDIX C: POWER SPECTRAL DENSITY CURVES

December 19, 2019

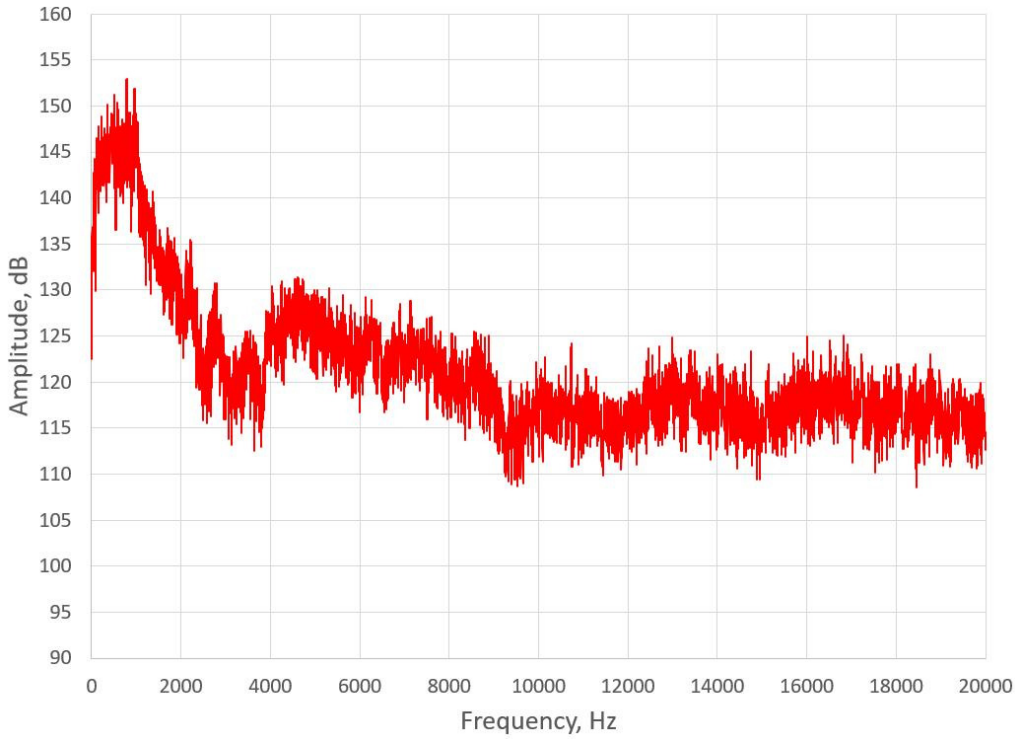

Figure C1: Power Spectral Density for the WM5a monitoring location on December 19, 2019

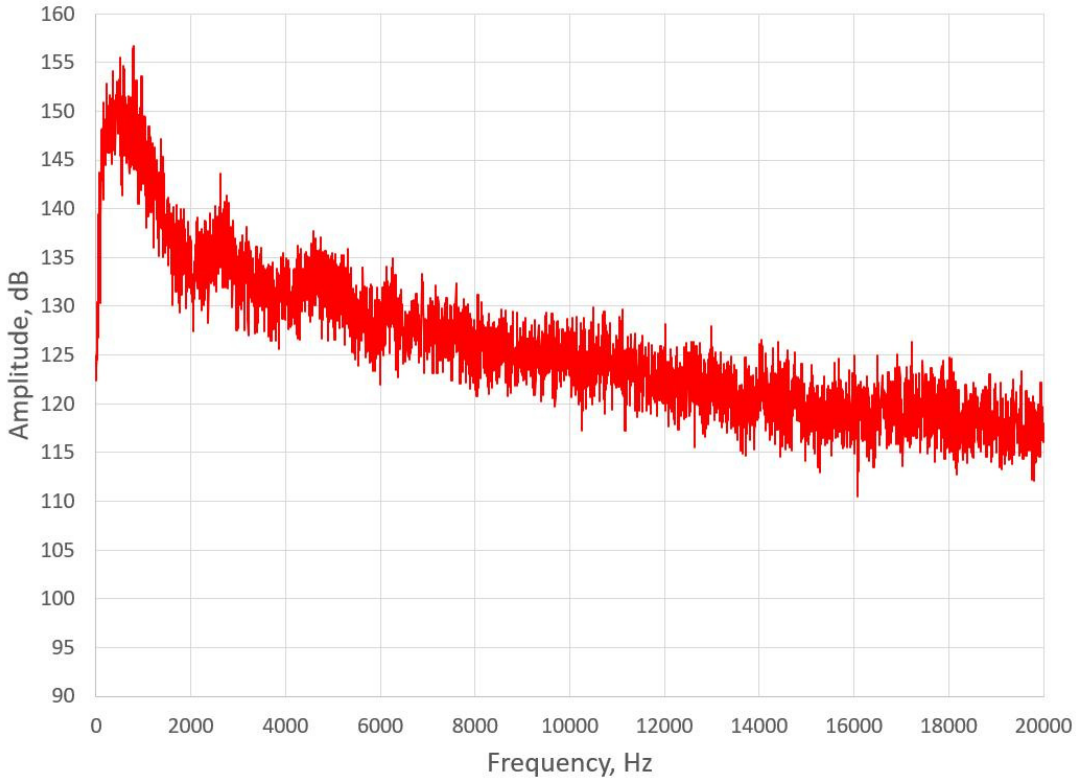

Figure C2: Power Spectral Density for the WM5b monitoring location on December 19, 2019

December 20, 2019

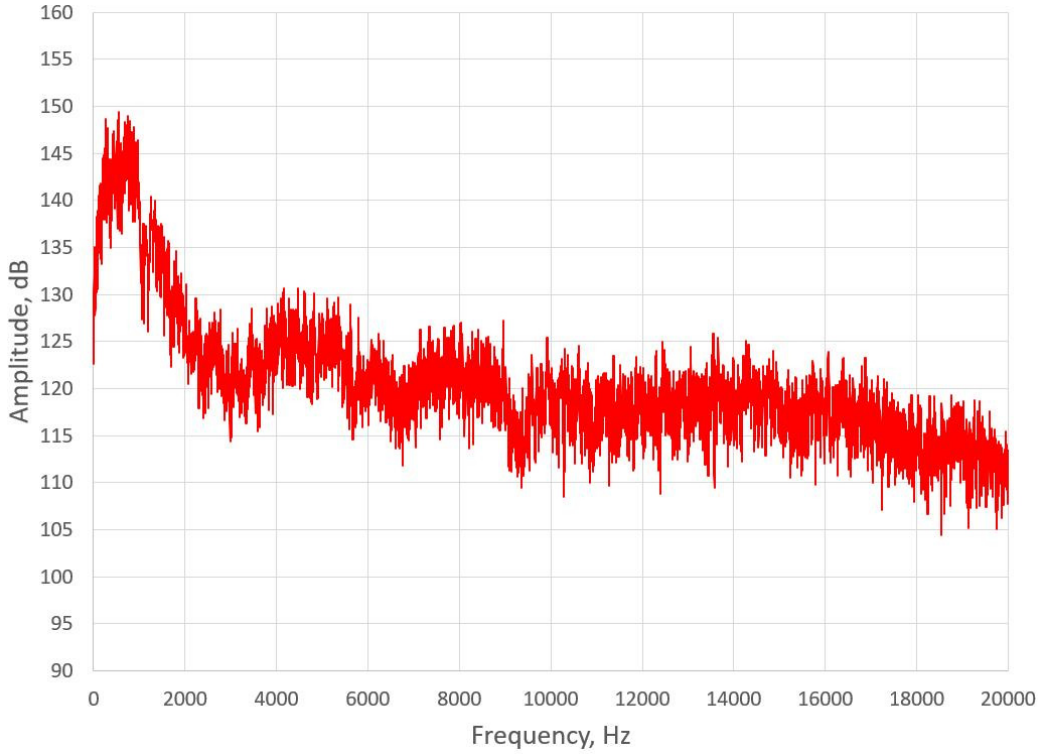

Figure C3: Power Spectral Density for the WM5 monitoring location on December 20, 2019

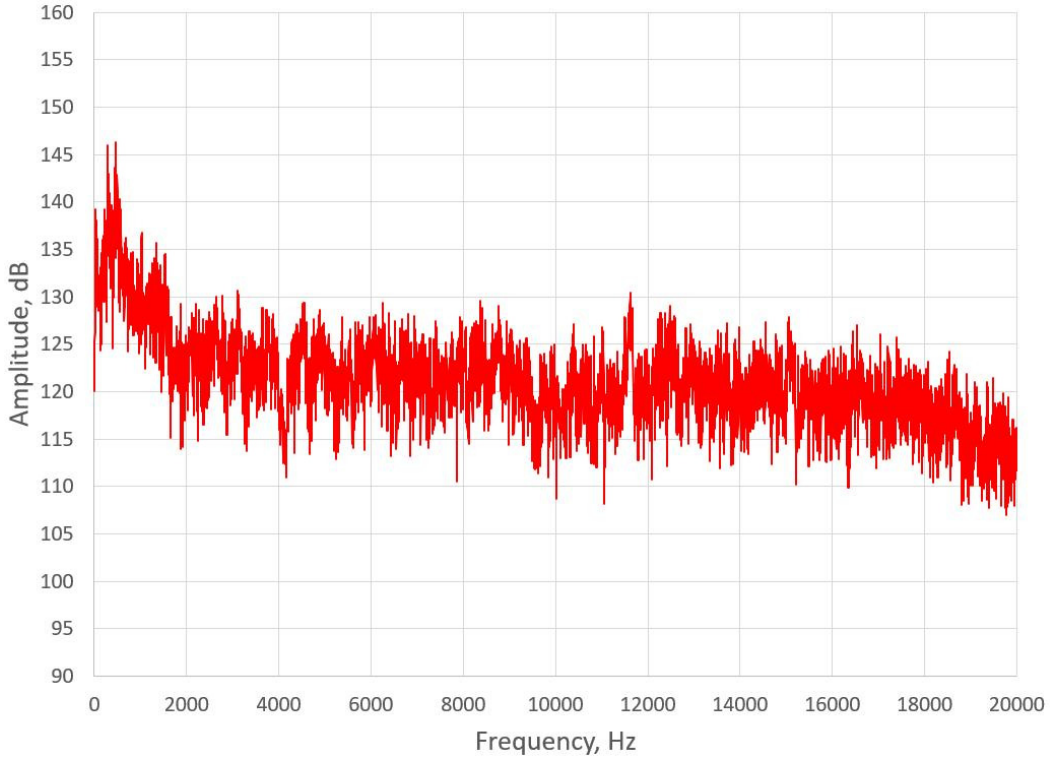

Figure C4: Power Spectral Density for the WM6 monitoring location on December 20, 2019